

INCREASE – *Increasing the penetration of renewable energy sources in the distribution grid by developing control strategies and using ancillary services*

D3.1 - Dynamic equivalent models for the simulation of controlled DRES



INCREASE

INCREASING THE PENETRATION OF RENEWABLE
ENERGY SOURCES IN THE DISTRIBUTION GRID BY
DEVELOPING CONTROL STRATEGIES AND USING
ANCILLARY SERVICES

D3.1 - Dynamic equivalent models for the simulation
of controlled DRES

INCREASE – *Increasing the penetration of renewable energy sources in the distribution grid by developing control strategies and using ancillary services*

D3.1 - Dynamic equivalent models for the simulation of controlled DRES

Document info

Project Number	608998 – INCREASE
Funding Scheme	Collaborative Project
Work Programme	Topic ENERGY.2013.7.1.1: Development and validation of methods and tools for network integration of distributed renewable resources
Number	D3.1
Title	Dynamic equivalent models for the simulation of controlled DRES
Dissemination Level	
Date	07.12.2014
Nature	
Authors	Andreas I. Chrysochos (AUTH), Georgios C. Kryonidis (AUTH), Eleftherios O. Kontis (AUTH), Charis S. Demoulias (AUTH), Grigoris K. Papagiannis (AUTH)
Contributors	
Reviewers	Bart Meersman, UGent Andrej Gubina, UL

Document History

Date	Authors	Action	Status
07/12/2014	Andreas I. Chrysochos Georgios C. Kryonidis Eleftherios O. Kontis Charis S. Demoulias Grigoris K. Papagiannis	Preparation of the 1st draft	
31/12/2014	Andreas I. Chrysochos Georgios C. Kryonidis Eleftherios O. Kontis Charis S. Demoulias Grigoris K. Papagiannis	Final version	

INCREASE – *Increasing the penetration of renewable energy sources in the distribution grid by developing control strategies and using ancillary services*

D3.1 - Dynamic equivalent models for the simulation of controlled DRES

Comments

This deliverable report corresponds to Task 3.1 – ‘Development of the principle modelling units for the integrated simulation platform’.

Contents

Document info	2
Document History.....	2
Comments.....	3
List of tables.....	6
List of figures.....	7
List of symbols and abbreviations	9
1. Introduction.....	10
1.1. Context	10
1.2. Goals.....	11
1.3. Report outline	11
2. Current practice in the simulation of distribution networks with controlled DRESs	13
2.1. Software tools based on time-domain solutions	13
2.2. Software platforms based on phasor-domain solution	14
2.3. Requirements for a complete simulation platform	14
3. The INCREASE simulation platform	16
3.1. Overview.....	16
3.2. General architecture	17
3.3. Tool components.....	18
3.3.1. Core platform.....	18
3.3.2. Draw tool.....	19
3.3.3. OpenDSS simulator	23
3.3.4. JADE environment.....	25
3.3.5. OMNeT++ simulator.....	25
3.4. Numerical validation and performance	25
3.4.1. Power flow accuracy in LV network.....	25
3.4.2. Power flow accuracy in MV network.....	27

INCREASE – *Increasing the penetration of renewable energy sources in the distribution grid by developing control strategies and using ancillary services*

D3.1 - Dynamic equivalent models for the simulation of controlled DRES

3.4.3.	Power flow accuracy in pilot installation	29
3.4.4.	Numerical accuracy in significantly unbalanced loading conditions	31
3.4.5.	Numerical performance in the presence of controllable DG units	33
4.	Implementation of Local Control.....	35
4.1.	Introduction.....	35
4.2.	Local Control formulation	35
4.2.1.	Droop control.....	35
4.2.2.	Voltage unbalance mitigation.....	36
4.3.	Core and OpenDSS algorithms of Local Control.....	38
4.4.	Numerical performance and accuracy considerations	41
5.	Simulation results	43
5.1.	Test case 1 – LV network.....	43
5.1.1.	Results of Local Control	44
5.1.2.	Investigation of different control schemes.....	46
5.2.	Test case 2 – MV network	50
5.2.1.	Results of Local Control	52
5.2.2.	Investigation of different control schemes.....	53
5.3.	Test case 3 – Elektro Gorenjska pilot installation	56
5.3.1.	Results of the Local Control	58
5.3.2.	Investigation of different control schemes.....	59
5.4.	Test case 4 – Stromnetz Steiermark pilot installation	63
5.4.1.	Investigation of different control schemes.....	64
6.	Conclusion	67
	References	69

List of tables

Table 3-1: DRESs power	26
Table 3-2: Total feeder unbalanced load.....	26
Table 3-3: Distribution transformer characteristics	26
Table 3-4: DG rated powers.....	27
Table 3-5: Aggregated loads	28
Table 3-6: Distribution transformer characteristics	28
Table 3-7: Total unbalanced load	30
Table 3-8: Inverters rated power.....	31
Table 3-9: Distribution transformer characteristics	31
Table 3-10: Relative differences (%) of power flow results in various nodes	31
Table 3-11: Line characteristics	32
Table 3-12: Transformer characteristics.....	32
Table 3-13: Power flow voltage results	32
Table 3-14: Power flow current results	32
Table 3-15: Characteristics of the lines	34
Table 3-16: Generation and consumption units.....	34
Table 3-17: Characteristics of the transformer	34
Table 3-18: Injected real power of DGs	34
Table 5-1: Inverters rated power.....	44
Table 5-2: Total feeder unbalanced load.....	44
Table 5-3: Distribution transformer characteristics	44
Table 5-4: DG rated powers.....	51
Table 5-5: Aggregated loads	51
Table 5-6: Distribution transformer characteristics	51
Table 5-7: Inverters rated power.....	57
Table 5-8: Distribution transformer characteristics	57
Table 5-9: Total aggregated load at Main Bus.....	64
Table 5-10: Rated powers of single-phase conventional inverters.....	64
Table 5-11: Rated powers of three-phase controllable inverters	64

List of figures

Fig. 2.1: Software classification	13
Fig. 3.1: Overview of the INCREASE simulation platform.....	18
Fig. 3.2: Main window of Draw library.	20
Fig. 3.3: GUI of slack bus	21
Fig. 3.4: GUI of bus.....	21
Fig. 3.5: GUI of line/cable	21
Fig. 3.6: GUI of constant load	21
Fig. 3.7: GUI of ZIP model	21
Fig. 3.8: GUI of transformer	21
Fig. 3.9: GUI of generator	21
Fig. 3.10: GUI of controllable inverter	22
Fig. 3.11: GUI of agent	22
Fig. 3.12: Example of a LV network designed in Draw	22
Fig. 3.13: OpenDSS solution scheme	24
Fig. 3.14: LV network topology	25
Fig. 3.15: Voltage profile along the LV network topology	26
Fig. 3.16: MV network topology	27
Fig. 3.17: Voltage profile of the first MV feeder.....	28
Fig. 3.18: Voltage profile of the second MV feeder	29
Fig. 3.19: Voltage profile of the third MV feeder	29
Fig. 3.20: Elektro Gorenjska network topology designed in Draw	30
Fig. 3.21: Simplified MV/LV network.....	32
Fig. 3.22: LV feeder with controllable DG units.....	33
Fig. 3.23: Droop curve of controllable DG unit.....	34
Fig. 3.24: Voltage profile along the LV feeder	35
Fig. 4.1: Droop curve of controllable DG units	36
Fig. 4.2: Damping conductance regions.....	38
Fig. 4.3: Main components interaction	39
Fig. 4.4: Local Control flowchart: a) Main routine and b) inverter implementation.....	40
Fig. 4.5: Numerical oscillations on the calculation of grid voltage.....	42
Fig. 5.1: LV network topology	44
Fig. 5.2: Injected real power of inverter 8	45
Fig. 5.3: Detail of convergence rate for inverter 8	45
Fig. 5.4: Injected real power of inverters	46
Fig. 5.5: Voltage profile along the LV feeder	46
Fig. 5.6: Total inverter injected power for different control schemes.....	47

Fig. 5.7: Total power losses for different control schemes	48
Fig. 5.8: Voltage profile of phase A for different control schemes	48
Fig. 5.9: Voltage profile of positive-sequence for different control schemes.....	49
Fig. 5.10: Voltage unbalance factor of zero-sequence along the LV feeder	50
Fig. 5.11: Voltage unbalance factor of negative-sequence along the LV feeder	50
Fig. 5.12: MV network topology	51
Fig. 5.13: Voltage profile of the first MV feeder.....	52
Fig. 5.14: Voltage profile of the second MV feeder	52
Fig. 5.15: Voltage profile of the third MV feeder	53
Fig. 5.16: Total inverter injected power for different control schemes.....	54
Fig. 5.17: Total power losses for different control schemes	54
Fig. 5.18: Positive-sequence voltage profile of first MV feeder	55
Fig. 5.19: Positive-sequence voltage profile of second MV feeder.....	55
Fig. 5.20: Positive-sequence voltage profile of third MV feeder.....	55
Fig. 5.21: Elektro Gorenjska network topology designed in Draw	56
Fig. 5.22: Total real load power	57
Fig. 5.23: Total reactive load power	57
Fig. 5.24: Injected real power of the inverters vs time	58
Fig. 5.25: Voltage of phase A for all inverters vs time	58
Fig. 5.26: Voltage of phase B for all inverters vs time	59
Fig. 5.27: Voltage of phase C for all inverters vs time	59
Fig. 5.28: Positive-sequence voltage for inverter 3 vs time	60
Fig. 5.29: Voltage of phase B for inverter 3 vs time	60
Fig. 5.30: Voltage unbalance factor of zero-sequence for inverter 3 vs time	61
Fig. 5.31: Voltage unbalance factor of negative-sequence for inverter 3 vs time	61
Fig. 5.32: Total inverter injected power for different control schemes vs time	62
Fig. 5.33: Total apparent power losses for different control schemes vs time.....	62
Fig. 5.34: Energienetze Steiermark network topology	63
Fig. 5.35: Total inverter injected power for different control schemes.....	65
Fig. 5.36: Total power losses for different control schemes	65
Fig. 5.37: Positive-sequence voltage levels for different control schemes.....	66
Fig. 5.38: Voltage unbalance factor of zero-sequence for different control schemes.....	66
Fig. 5.39: Voltage unbalance factor of zero-sequence for different control schemes.....	66

INCREASE – *Increasing the penetration of renewable energy sources in the distribution grid by developing control strategies and using ancillary services*

D3.1 - Dynamic equivalent models for the simulation of controlled DRES

List of symbols and abbreviations

Symbol	Description	Symbol	Description
P_{nom}	Nominal (rated) power of inverter	g_1	Fundamental input conductance
u_g	Voltage at the connection point	u_a, u_b, u_c	Phase voltage magnitudes
P_{inj}	Injected active power	$\vartheta_a, \vartheta_b, \vartheta_c$	Phase voltage angles
P_{ref}	Reference power of the control inverter	g_d	damping conductance
u_{cdb}	Constant damping band	$\underline{u}_0, \underline{u}_1, \underline{u}_2$	zero-, positive- and the negative-sequence components of the grid voltage
u_{max}	Maximum allowable voltage in the grid as defined by the corresponding standards	u_{cpb}	Constant power band voltage
u_{min}	Minimum allowable voltage in the grid as defined by the corresponding standards	k	Integral term
AG	Agent	LV	Low-Voltage
D	Deliverable	MAS	Multi-Agent System
DG	Distributed Generation	MV	Medium-Voltage
DRES	Distributed Renewable Energy Source	PCC	Point of Common Coupling
DSO	Distribution System Operator	pu	per unit
EPRI	Electric Power Research Institute	TSO	Transmission System Operator
GUI	Graphical User Interface	VUF	Voltage Unbalance Factor
HV	High-Voltage	WP	Work Package

INCREASE – *Increasing the penetration of renewable energy sources in the distribution grid by developing control strategies and using ancillary services*

D3.1 - Dynamic equivalent models for the simulation of controlled DRES

1. Introduction

1.1. Context

The INCREASE project focuses on intelligent ways to manage distributed renewable energy sources (DRES) in low- (LV) and medium-voltage (MV) networks. This is achieved by providing ancillary services, including voltage control, line congestion and provision of reserves, towards distribution (DSOs) and transmission system operators (TSOs). The cornerstone of the project activities is the introduction of inverter-interfaced DRES that enable high flexibility and advanced features, further supported by an intelligent multi-agent-based control strategy with enhanced structure and algorithms. INCREASE aims at providing solutions for operational problems in power systems, following the integration of variable DRES as well as for the prosumers using advanced technological solutions and intelligent control strategies.

Under the INCREASE framework, and especially in Work Package (WP) 3, a supporting simulation platform will be developed, allowing for the design, analysis, and optimization of the developed solutions. This simulation platform will be a valuable tool for DSOs in order to investigate the influence of DRES on their distribution grids, implementing either the INCREASE proposed solutions or any other similar control scheme. The simulation platform will be developed on existing open-source software and will include the following major features:

- Simulation of the asymmetric distribution system (both LV and MV networks) with the presence of unbalanced loads.
- Integration of the locally controlled, inverter-interfaced, distributed generation (DG) units, i.e. of the Local Control scheme for overvoltage and voltage unbalance mitigation.
- Incorporation of a Multi-Agent System (MAS) taking into account the multi-objective Overlay and Scheduling Control algorithms.
- Implementation of a communication network simulator for the evaluation of the existing infrastructure and the communication requirements for the MAS control system.

The software platform architecture will also allow the integration of other external and independent software modules, such as forecasting algorithms, demand side management, demand response, and constraint optimization tools.

INCREASE – *Increasing the penetration of renewable energy sources in the distribution grid by developing control strategies and using ancillary services*

D3.1 - Dynamic equivalent models for the simulation of controlled DRES

1.2. Goals

In this report, the overall architecture and some components of the developed simulation platform are presented. Specifically, the graphical user interface (GUI) is first described, in which any LV or/and MV power system can be readily designed and configured. The GUI models of typical power system elements as well as of the developed controllable inverters and agents are shown, whereas their input interface is also thoroughly presented using descriptive mock screens. The validity of the power flow scheme incorporated in the INCREASE simulation platform is also examined, by comparing it to other commercial and open-source programs in various LV and MV networks. In all cases it is found that the adopted power flow routine is very accurate and numerically efficient.

Next, the implementation of Local Control is presented, focusing on its numerical robustness and performance. Simulation results are presented from different test cases, selected to represent typical distribution grid configurations in both LV and MV levels, as well as from the selected pilot installations. All results show the efficiency of the proposed Local Control in overvoltage and voltage unbalance mitigation, compared to other conventional control schemes. The analysis is extended by assuming two different voltage criteria for the Local Control of inverters, checking their performance in overvoltage and voltage unbalance mitigation. The other components of the INCREASE simulation platform are only briefly introduced, since they will be extensively described in the next two Deliverables of WP3, namely in D3.2 and D3.3.

1.3. Report outline

This introductory chapter is followed by:

Chapter 2: Current practice in the simulation of distribution grids with controlled DRESs. The most common practices in the simulation of distribution networks are described with special emphasis on their numerical performance. Various technical and numerical issues are highlighted, focusing on the simulation accuracy and numerical efficiency, especially in cases where dynamic models and controlled DRESs are included.

Chapter 3: The INCREASE simulation platform. The overall structure and the individual components of the INCREASE simulation platform are described. The report focuses on the development of GUI and on the software tools needed for the implementation of the core solution algorithms as well as of the Local Control.

Chapter 4: Implementation of Local Control. The Local Control described in Deliverable D2.4 is incorporated in the INCREASE simulation platform for overvoltage and voltage unbalance mitigation. The integrated model is slightly modified compared to the D2.4 model

INCREASE – *Increasing the penetration of renewable energy sources in the distribution grid by developing control strategies and using ancillary services*

D3.1 - Dynamic equivalent models for the simulation of controlled DRES

with the introduction of an integral term in the power output of controllable inverters, to enhance the overall numerical stability and performance of the model.

Chapter 5: Simulation results. Simulation results from various test cases and pilot installations are presented, revealing the effectiveness of the proposed Local Control. Results are compared with the corresponding results from conventional control methods, whereas a detailed investigation of the numerical performance is also carried out.

Chapter 6: Conclusion. General conclusions are drawn and a plan for the next research steps is proposed.

2. Current practice in the simulation of distribution networks with controlled DRESs

Over the past decades, research has been focused on developing software tools to analyze, plan, optimize and simulate electrical networks. The advent of DG has gradually changed the power delivery system from downstream unidirectional to a bidirectional scheme, introducing challenging technical issues, such as unacceptable overvoltages, voltage unbalances, line congestions, and protection issues. Although novel control schemes, e.g. droop control, have been proposed for interfacing DGs to the grid and mitigating these issues, such controlled inverters need to be also efficiently incorporated in the simulation software packages [1], [2].

Considering the simulation of power system networks, the existing open source and commercial software products can be divided into the two main categories of Fig. 2.1, according to the adopted solution method.

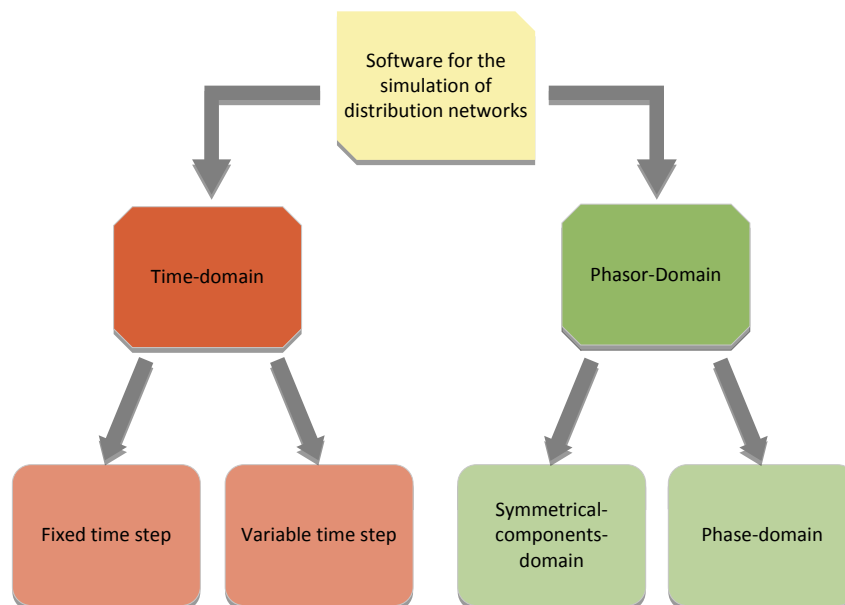


Fig. 2.1: Software classification

2.1. Software tools based on time-domain solutions

In this category, the power system network is simulated explicitly in time-domain by solving the differential equations that describe all power system components. Libraries and separate modules for modeling and simulating electrical power systems are also available, whereas unbalanced power flow calculations and detailed harmonic analyses can also be executed. Due to the time-domain solution method and the nature of each problem, different solver types must be chosen, which can generally use fixed or variable solution

INCREASE – *Increasing the penetration of renewable energy sources in the distribution grid by developing control strategies and using ancillary services*

D3.1 - Dynamic equivalent models for the simulation of controlled DRES

time steps. Although these simulation tools provide the ability to integrate DG control schemes in a very straightforward manner, they cannot be used for the simulation of extended networks, due to the excessive execution times resulting by the small time steps needed for the numerical integration of the differential equations [3].

A representative software of this category is SIMULINK/SimPowerSystems [4], which offers various capabilities for the simulation of electrical power systems, incorporating also tools that can be used to develop control systems. Although SIMULINK suffers from the drawbacks reported previously, it is a very reliable tool in verifying the performance of detailed models and as such has been also used in this Deliverable.

2.2. Software platforms based on phasor-domain solution

In this category, simplified algebraic equations are used for the simulation of power systems operating in a steady-state condition. As a result, power flow and harmonic analysis calculations can be readily performed in small execution times even in cases of extended networks. The major drawback of such models is that their core calculation routines may become cumbersome with the incorporation of DG droop controls or of other additional control schemes [5].

In cases of asymmetrical network operation, the phasor calculation can be performed either in symmetrical-components- or in phase-domain. The former approach is based on transformations from phase- to symmetrical-components-domain and vice versa. This transform can occasionally introduce small round-off errors in the calculation procedure and thus can lead to erroneous results [6], [7]. Most commercial software platforms are using this approach [8], [9].

On the other hand, the more complicated phase-domain approach employs full multi-phase circuit models for all power system components and can solve extended unbalanced networks with high accuracy. OpenDSS is a representative open-source software of this category, able to solve quasi-static power flows, harmonics and dynamics [5], [10]. Its superior performance and flexibility lies in its fast and robust calculation routine, which can be also driven by a variety of software tools [7].

2.3. Requirements for a complete simulation platform

Most of the commercially available software platforms allow the use of customisable configurations than can cover all electrical aspects in transmission, distribution, and generation, including steady-state calculations, power quality optimization and protection coordination. Although originally developed for high-voltage (HV) and MV grids as well as LV installations, most of them are updated to simulate efficiently also LV distribution grids

INCREASE – *Increasing the penetration of renewable energy sources in the distribution grid by developing control strategies and using ancillary services*

D3.1 - Dynamic equivalent models for the simulation of controlled DRES

including DGs. However, a major drawback is that almost all of them have a closed form architecture, not allowing the easy and efficient integration of user developed models, especially regarding control systems.

Therefore it is evident that a new simulation platform should be developed within the INCREASE project, comprising the benefits of both software categories and allowing the integration of the developed DRES control strategies. The new simulation tool should have the following basic characteristics:

- Use of phasor-domain solutions to have short execution times even in cases of extended distribution networks. Since unbalance mitigation is one of the main benefits of the proposed control scheme, phase-domain approach is selected, since it yields more accurate results in the cases of heavily unbalanced power system configurations.
- The ability to be driven from external software tools in order to allow the efficient incorporation of any DG control scheme.

Furthermore to be compatible with the design of modern power systems and smart grids, the INCREASE simulation platform should also incorporate other advanced features, such as:

- A GUI tool for the convenient input and configuration of the system under study.
- The ability to be interlinked with other software platforms and tools in order to develop a generic co-simulation platform, able to simulate modern power system networks from both power system and communication point of view.

INCREASE – *Increasing the penetration of renewable energy sources in the distribution grid by developing control strategies and using ancillary services*

D3.1 - Dynamic equivalent models for the simulation of controlled DRES

3. The INCREASE simulation platform

3.1. Overview

The main goal of the INCREASE simulation platform is to analyze MV/LV electrical power grids, including all potential DRES, DGs, loads and control systems. Due to the required analysis over extended observation times, a quasi-dynamic solution is preferred over detailed dynamic simulations, since it can offer a better insight of the system steady-state conditions and needs significantly smaller total execution times. This type of solution is based on sequential steady-state power flow calculations over a user-defined time span with a variable time step. As a result, the simulation algorithm must be able to handle unbalanced AC power flow calculations, preferably solved using phase-domain approach, as well as quasi-dynamic profile-based load flow calculations [6], [11], [12].

Furthermore, due to the lack of available data for the network topology and/or network operating conditions, reduced equivalent models for both passive and active parts of the extended distribution networks are also provided [13], [14].

- In case of purely passive network parts, including only different load types, the system dynamic behavior can be approximated by implementing either constant power or voltage dependent quasi-dynamic elements (e.g. ZIP). In the later case, loads are described with data sets of real and reactive power as well as voltage against time at their connection points [15], [16]. These data sets can be further correlated in order to derive the equivalent equations or data sets of real and reactive power against voltage.
- In case of active network parts, i.e. presence of DRES and loads, reduced order models can be built using the complex black- or gray-box techniques [17]-[20]. These models are based on detailed time-series of measurements for real and reactive power as well as for voltage magnitude and angle at the boundary busbars to determine the structure of the system beyond that point [21]. However, when the modeling of specific active networks is not critical, the time series of recorded data can be further simplified, permitting the use of an approach similar to the ZIP/exponential static load modeling described above.

The three developed control schemes are also fully integrated in the INCREASE simulation platform and are solved together with the other network models. Specifically:

- The first level control, known as Local Control, is associated with the controllable inverters for overvoltage and voltage unbalance mitigation [22]-[25]. It continuously

INCREASE – *Increasing the penetration of renewable energy sources in the distribution grid by developing control strategies and using ancillary services*

D3.1 - Dynamic equivalent models for the simulation of controlled DRES

works, adjusting the total amount of the inverter real power output and its distribution among the three phases according to the voltage at the Point of Common Coupling (PCC).

- The second level control, known as Overlaying Control, is related to the MAS coordination algorithms for the application of specific control strategies focused on voltage control and line congestion management [26]. It is an event-driven control, able to change various aspects of the Local Control system, such as the slopes of the inverter droop curves and the corresponding set-points.
- The third level control, known as Scheduling Control, addresses problems on a longer time scale. This control focuses on power loss reduction, maximizing real power injection and optimizing the performance according to predefined criteria and constraints which also involve load and generation forecasting data.

Finally, the INCREASE simulation platform employs a discrete event simulator of communication networks in order to evaluate the communication performance of the MAS control system. This simulator is able to analyze possible contingencies of the communication infrastructure on the operation of the MAS control system. It can also be used to investigate alternative options on the design of the necessary infrastructure and to examine the communication system vulnerability and its impact on the control system performance.

3.2. General architecture

In Fig. 3.1 the overview of the supporting simulation platform is presented, allowing the design, analysis and optimization of the developed solutions. The INCREASE simulation platform consists of different open-source tool components and of their mutual interconnections. Specifically, the developed software includes:

- The Core platform, which is the base of the simulation software and interconnects the different tool components. Moreover, it is the base for the implementation of Local Control.
- The Draw tool, a graphical pre-processor with design and import/export capabilities to allow the user-friendly input and configuration of the distribution or transmission network under investigation.
- The OpenDSS environment [10], which is a phasor-domain grid simulator, able to handle unbalanced power flow problems and also allowing the implementation of the necessary power system component models as well as of the required reduced equivalent models.

INCREASE – *Increasing the penetration of renewable energy sources in the distribution grid by developing control strategies and using ancillary services*

D3.1 - Dynamic equivalent models for the simulation of controlled DRES

- The JADE environment [27], which is a high-level language implementing the Overlaying and Scheduling Control algorithms as well as the communication among the MAS.
- The OMNeT++ simulator [28], which is a dedicated tool for the evaluation of the communication infrastructure performance of the system under study.

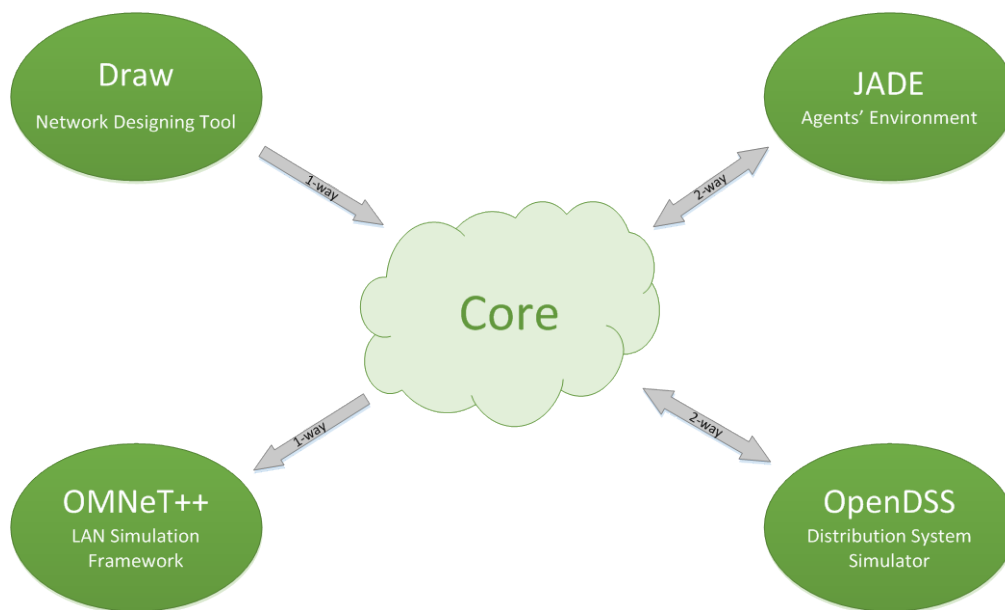


Fig. 3.1: Overview of the INCREASE simulation platform.

3.3. Tool components

3.3.1. Core platform

The Core platform is developed in MATLAB, which is a high-level language and interactive environment, suitable for numerical computations, visualization, and programming [29]. In the framework of the INCREASE simulation platform, the initial GUI windows for defining the main simulation parameters, as well as the post-processing tools for results are implemented within the Core.

Furthermore, the Core is responsible for the implementation of the interconnections between the different components of the INCREASE simulation platform, as shown in Fig. 3.1. Specifically, there are the following 4 interconnections among the key elements of the platform:

1. An one-way interconnection between Core and Draw. This link transfers all necessary data from the Draw input pre-processor to variables and structures in Core. The pre-processor also includes necessary algorithms to categorize all power system

INCREASE – *Increasing the penetration of renewable energy sources in the distribution grid by developing control strategies and using ancillary services*

D3.1 - Dynamic equivalent models for the simulation of controlled DRES

elements and to list the corresponding nodes, thus creating the necessary graph matrices which are crucial for the correct function of all other platform components.

2. A two-way interconnection between Core and OpenDSS. This interaction is based on the well-known COM interface, transferring all necessary input files to the OpenDSS simulator (.dss files). Additionally, the corresponding results from the simulations performed in OpenDSS are sent back to Core via the same interconnection.
3. A two-way interconnection between Core and JADE. This interaction allows the communication of MAS components with the core of the INCREASE platform, transmitting the required data, e.g. grid topology and operational state, agent locations, messages, set points, and possible communication delays, for the configuration of the various agents according to the predefined overlaying or scheduling control schemes. The outcome of the agents returns to the Core through this connection, in order to change various aspects of the Local Control system, responding to the control actions implemented by the MAS.
4. A one-way interconnection between the Core and OMNeT++. This connection is responsible for the transmission of the necessary data to define the grid and MAS structure, as well as to create the corresponding input files of the LAN simulator (.ned and .ini files).

Finally, the implementation of Local Control is also performed in the Core platform. A detailed description of the control algorithms and their implementation in the INCREASE simulation platform is presented in Chapter 4.

3.3.2. Draw tool

3.3.2.1. Main GUI components

The graphic library for the input of all individual network components is based on SIMULINK models and contains all components defined in the toolbox of Fig. 3.2. This collection includes all basic power system components, such as loads and generation units, as well as the more advanced models of controllable inverters and agents. All elements work in a drag and drop environment by simply putting them in the design area, configuring their required data, and making the appropriate connections.

INCREASE – *Increasing the penetration of renewable energy sources in the distribution grid by developing control strategies and using ancillary services*

D3.1 - Dynamic equivalent models for the simulation of controlled DRES

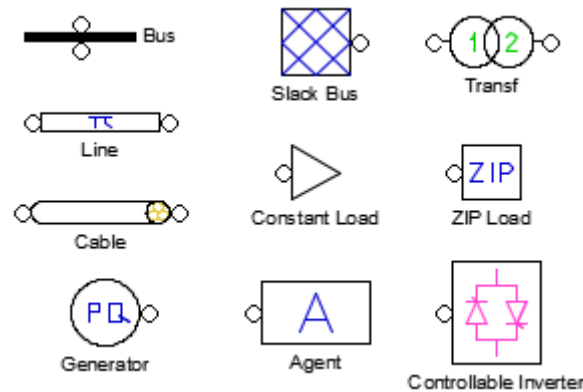


Fig. 3.2: Main window of Draw library.

3.3.2.2. Additional features

In the final version of the Draw component additional functions will be implemented, such as:

- The convenient incorporation of time-series data into the corresponding GUI elements. This will be done by accessing different text- or excel-based files that will include the necessary time-series of the generation and consumption data of DRESs and loads, respectively.
- A data conversion tool to provide basic import capabilities from file formats used in other simulation software packages and design environments to variables and structures compatible with the INCREASE simulation platform. This will be implemented by importing the text- or excel-type export files created by the majority of the available commercial or open-source software packages and reconstructing the topology and assigning the data parameters to the appropriate grid elements within the Core component of the INCREASE simulation platform.

3.3.2.3. Examples of GUI components

In Figs. 3.3-3.11 mock screens of the GUI windows for configuring the main power system components are presented, along with the necessary data that need to be defined by the user. All elements are also accompanied by brief help descriptions, when pressing the corresponding button. Finally, in Fig. 3.12 a complete example of an extended LV network is presented, as designed in Draw.

INCREASE – Increasing the penetration of renewable energy sources in the distribution grid by developing control strategies and using ancillary services
 D3.1 - Dynamic equivalent models for the simulation of controlled DRES

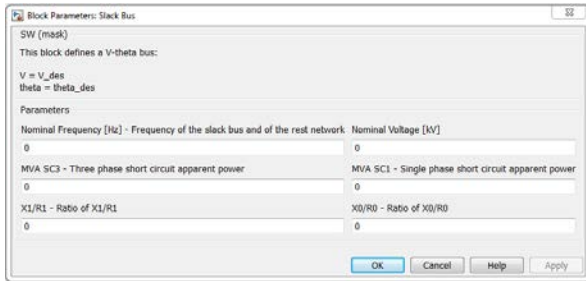


Fig. 3.3: GUI of slack bus

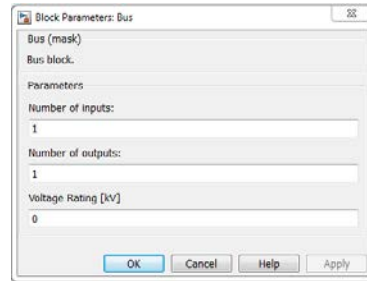


Fig. 3.4: GUI of bus

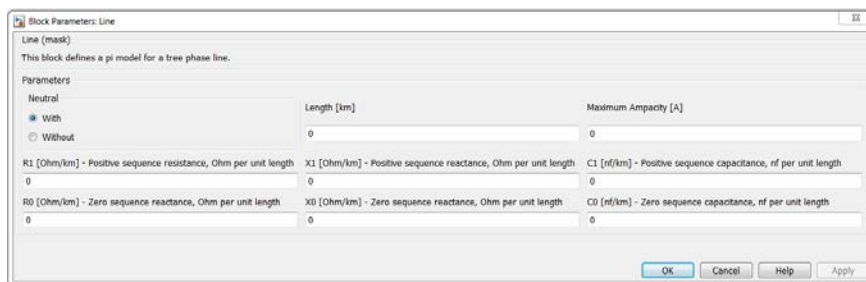


Fig. 3.5: GUI of line/cable



Fig. 3.6: GUI of constant load

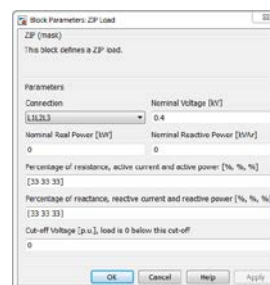


Fig. 3.7: GUI of ZIP model

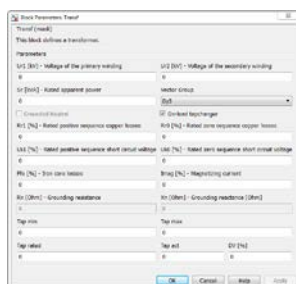


Fig. 3.8: GUI of transformer



Fig. 3.9: GUI of generator

INCREASE – *Increasing the penetration of renewable energy sources in the distribution grid by developing control strategies and using ancillary services*
 D3.1 - Dynamic equivalent models for the simulation of controlled DRES

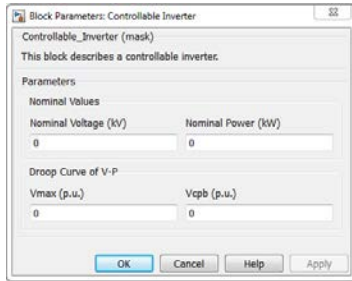


Fig. 3.10: GUI of controllable inverter

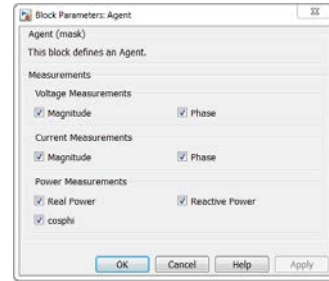


Fig. 3.11: GUI of agent

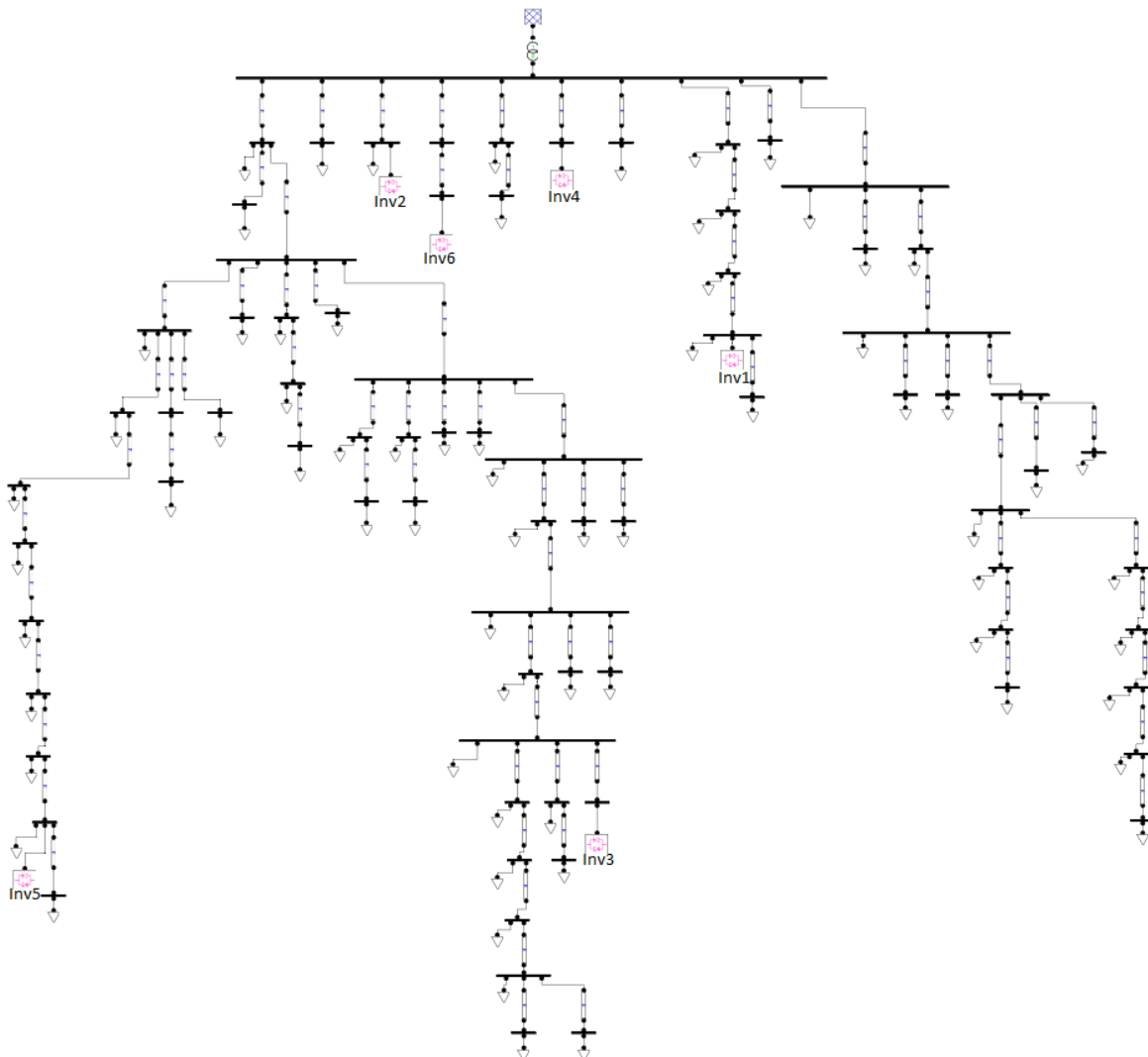


Fig. 3.12: Example of a LV network designed in Draw

INCREASE – *Increasing the penetration of renewable energy sources in the distribution grid by developing control strategies and using ancillary services*

D3.1 - Dynamic equivalent models for the simulation of controlled DRES

3.3.3. OpenDSS simulator

3.3.3.1. Overview

After the detailed categorization of the open-source and commercial software conducted in Deliverable D1.1, the OpenDSS simulation tool was selected as the power flow solver within the INCREASE simulation platform [30]. This was done, since OpenDSS provides all the advantages of an open-source software, while it also offers highly accurate results, remarkable numerical performance, and vast communication abilities with external programs.

More specifically, OpenDSS is a comprehensive, open-source simulation tool for electric utility distribution systems, developed and distributed by the Electric Power Research Institute (EPRI). The OpenDSS can be implemented as either a stand-alone executable program or an in-process COM server DLL, designed to be driven from a variety of existing software tools. Through the COM interface, the user is able to design and execute custom solution modes and features from an external program, and perform the functions of the simulator, including the definition of the model data. This provides powerful external analytical capabilities as well as excellent graphics for displaying results.

Furthermore, it offers the most common power system analysis algorithms for both steady-state and dynamic analyses. It also includes various quasi-dynamic solution modes, such as snapshot-daily-yearly power flows and harmonic analyses, which are ideal for sequential time simulations. The time period can be arbitrary selected, whereas users may also use external macros to drive the load models in some other manner. The results of a power flow generally include bus voltages, branch currents, grid losses, and other information available for the total system, for each component, and for certain defined areas.

3.3.3.2. Power flow calculation routine

Considering the power flow problem, the OpenDSS uses the full phase-domain circuit model. Specifically, the OpenDSS adopts a generalized admittance formulation of the examined circuit, as shown in Fig. 3.13. The primitive admittance (Y_{prim}) for each element in the circuit is created and these matrices are fed to the sparse matrix solver to construct the system admittance (Y) matrix. An initial data set for the voltages is obtained by performing a zero load power flow. The iteration cycle starts by obtaining the injection currents from all the power conversion elements in the system and adding them into the appropriate slots in the current (I) vector. The sparse set is then solved for the next estimation of the voltages,

INCREASE – *Increasing the penetration of renewable energy sources in the distribution grid by developing control strategies and using ancillary services*

D3.1 - Dynamic equivalent models for the simulation of controlled DRES

whereas the cycle repeats until the voltages solution obtained converge according to a user-defined tolerance.

The adopted iterative solution converges quickly for most distribution system configurations, thus it is preferred over other typical Newton-Raphson power flow methods that are usually performed in symmetric-component-domain. The system Y matrix is typically not rebuilt during the power flow process, thus the number of iterations is kept to a minimum and are performed in a very fast way. This is quite important mostly in cases where control techniques of DG units have to be incorporated with the power flow calculation scheme. Moreover, this calculation routine yields accurate results, unlike other commercial program platforms, which can introduce significant round-off errors.

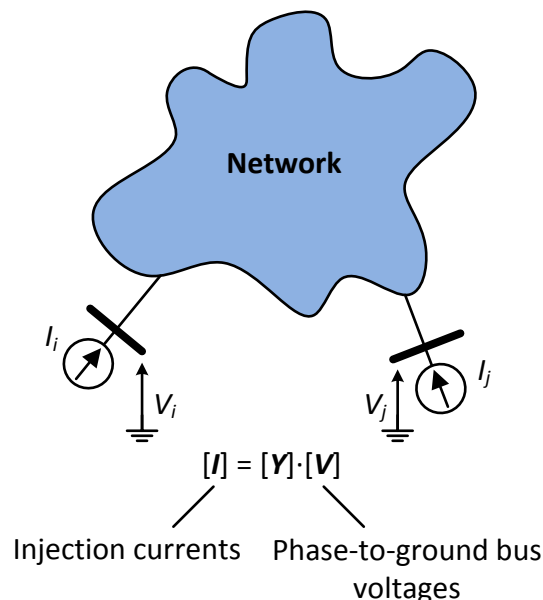


Fig. 3.13: OpenDSS solution scheme

3.3.3.3. Modeling capabilities

Apart from the accurate and efficient power flow calculation routine, OpenDSS offers great modeling capabilities for all types of power system networks. The fundamental circuit components are divided to passive grid components, e.g. lines, cables and transformers, and active grid elements, e.g. generators and loads. For all these elements, the bus and nodes necessary to represent the interconnected systems are dynamically created. Furthermore, multiphase terminals can be generally defined, which is quite important for the efficient implementation of generators with zero-sequence synchronous reactances and multi-winding transformers with arbitrary vector groups. Finally, the OpenDSS also includes

INCREASE – *Increasing the penetration of renewable energy sources in the distribution grid by developing control strategies and using ancillary services*

D3.1 - Dynamic equivalent models for the simulation of controlled DRES

various supporting algorithms for the definition of the basic line and cable data, the emulation of switched capacitors, and the regulation of transformer tap changers.

3.3.4. JADE environment

A detailed description of JADE environment will be included in the Deliverable D3.2 – ‘Integrated simulation platform which models the key components and control strategies’.

3.3.5. OMNeT++ simulator

A detailed description of OMNeT++ simulator will be included in the Deliverable D3.3 – ‘Report on simulation results and evaluation of the integrated simulation platform’.

3.4. Numerical validation and performance

To check the accuracy and the numerical efficiency of the INCREASE simulation platform a number of test cases have been examined, including MV/LV networks and various loading conditions. In all cases, results obtained by the OpenDSS component are compared to the corresponding of other representative commercial (NEPLAN [8], SIMULINK [29]) and/or open-source (PSAT [31]) software.

3.4.1. Power flow accuracy check in LV network

The test case of Fig. 3.14 consists of different loads and DRESs, connected to the LV feeder. The total power of the 9 DRESs and the total unbalanced load are shown in Tables 3-1 and 3-2, respectively. The 4-wire 3phase distribution lines have cross sections ranging from 4x16 mm² to 4x70 mm² with lengths varying from 10 m up to 100 m. A typical MV/LV distribution transformer is considered with the characteristics given in Table 3-3.

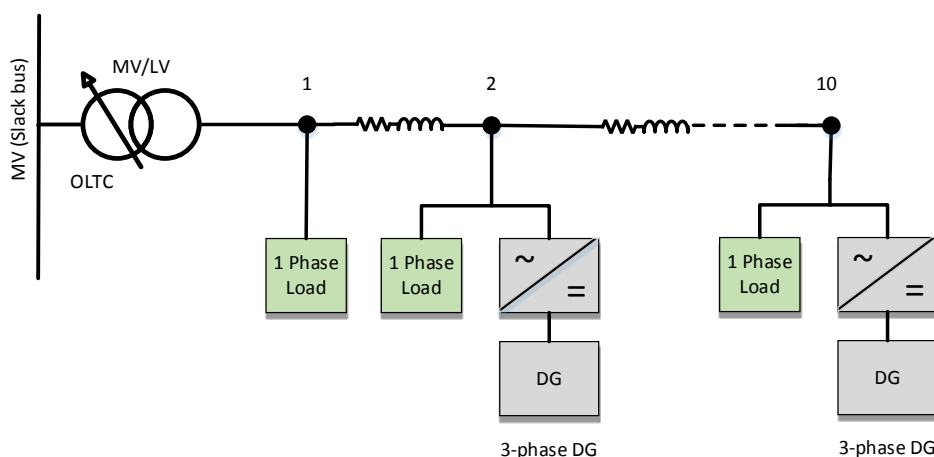


Fig. 3.14: LV network topology

INCREASE – Increasing the penetration of renewable energy sources in the distribution grid by developing control strategies and using ancillary services

D3.1 - Dynamic equivalent models for the simulation of controlled DRES

Table 3-1: DRESSs power

	Rated power (kVA)		Rated power (kVA)
DRES 1	5	DRES 6	10
DRES 2	10	DRES 7	5
DRES 3	5	DRES 8	15
DRES 4	8	DRES 9	10
DRES 5	10		

Table 3-2: Total feeder unbalanced load

	Real power (kW)	Reactive power (kVAr)
Phase A	38.8	10.8
Phase B	21	5.2
Phase C	23	3.6

Table 3-3: Distribution transformer characteristics

S_n (kVA)	U_n (kV)	Vector group	u_k (%)	No-load losses (W)	Rated load losses (W)
250	20 / 0.4	Dyn5	4	425	3250

In Fig. 3.15 the 3phase voltage magnitude in all grid nodes, obtained by OpenDSS, are compared with the corresponding of the NEPLAN software. Results are in excellent agreement in all phases, thus validating the power flow scheme of the OpenDSS component of the INCREASE simulation platform.

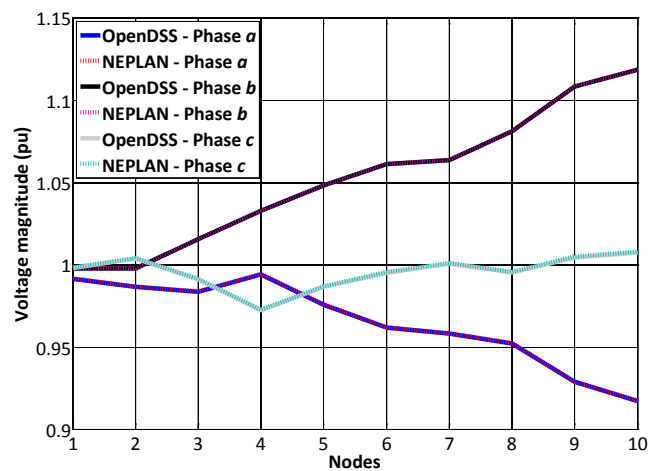


Fig. 3.15: Voltage profile along the LV network topology

INCREASE – Increasing the penetration of renewable energy sources in the distribution grid by developing control strategies and using ancillary services
 D3.1 - Dynamic equivalent models for the simulation of controlled DRES

3.4.2. Power flow accuracy check in MV network

The MV network of Fig. 3.16 consists of three feeders with segment lengths of 4 km and typical line cross-section of 50 mm². In Table 3-4 the aggregated rated apparent power of the 5 DG units connected along the MV feeders, is shown. In Table 3-5 the aggregated loads of all buses are given, all assumed fully balanced as connected directly to the MV branches. A typical HV/MV transformer is also considered with its characteristics given in Table 3-6.

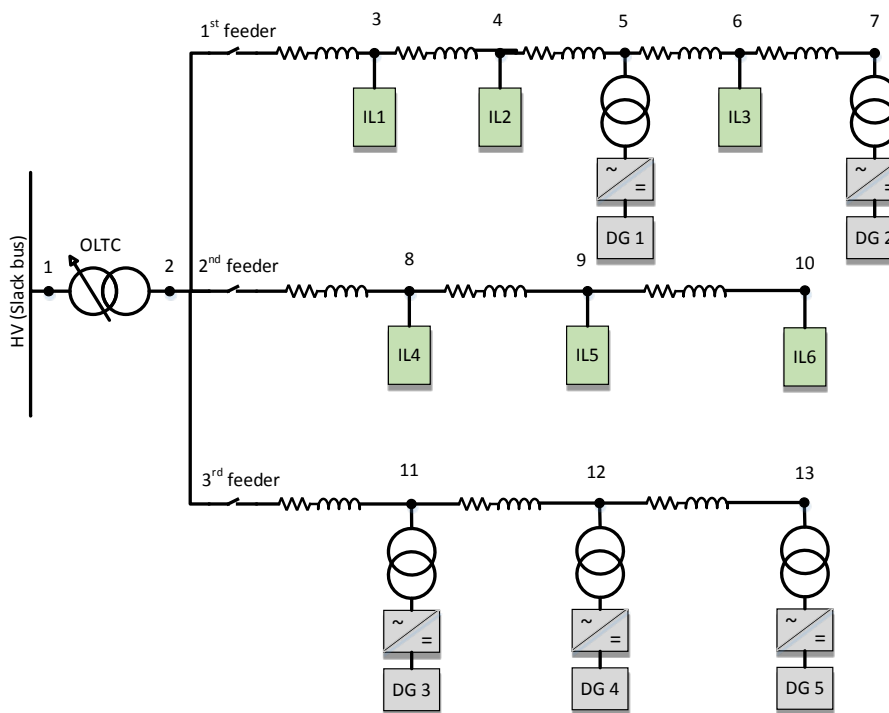


Fig. 3.16: MV network topology

Table 3-4: DG rated powers

	Rated Power (kVA)
DG 1	3500
DG 2	3500
DG 3	3300
DG 4	3300
DG 5	3300

INCREASE – Increasing the penetration of renewable energy sources in the distribution grid by developing control strategies and using ancillary services

D3.1 - Dynamic equivalent models for the simulation of controlled DRES

Table 3-5: Aggregated loads

	Real Power (kW)	Reactive Power (kVAr)
Bus 3	2330	1160
Bus 4	2330	1160
Bus 6	2330	1160
Bus 8	1400	700
Bus 9	1400	700
Bus 10	1400	700

Table 3-6: Distribution transformer characteristics

S_n (MVA)	U_n (kV)	Vector group	u_k (%)	No-load losses (kW)	On-load losses (kW)
50	150/ 20	Yd5	17.74	165	1250

The positive-sequence voltage profile along each MV feeder is presented Figs. 3.17-3.19, calculated by the OpenDSS, NEPLAN and PSAT software. A very good agreement between the power flow results is observed again, confirming the high accuracy of the OpenDSS tool component.

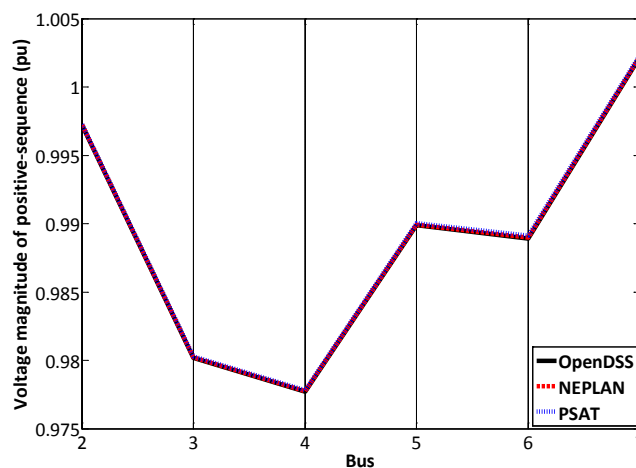


Fig. 3.17: Voltage profile of the first MV feeder

INCREASE – *Increasing the penetration of renewable energy sources in the distribution grid by developing control strategies and using ancillary services*

D3.1 - Dynamic equivalent models for the simulation of controlled DRES

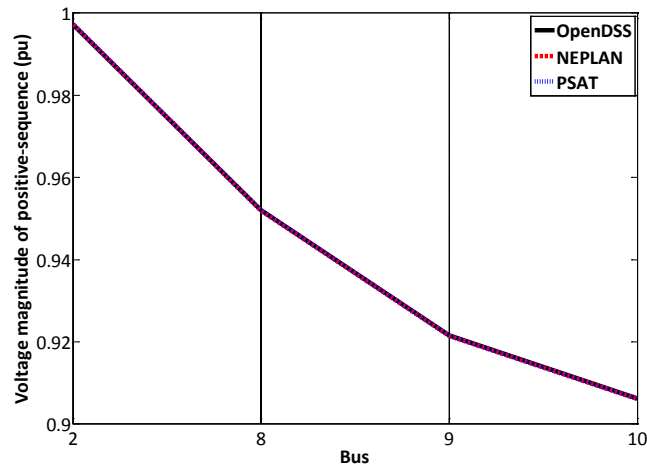


Fig. 3.18: Voltage profile of the second MV feeder

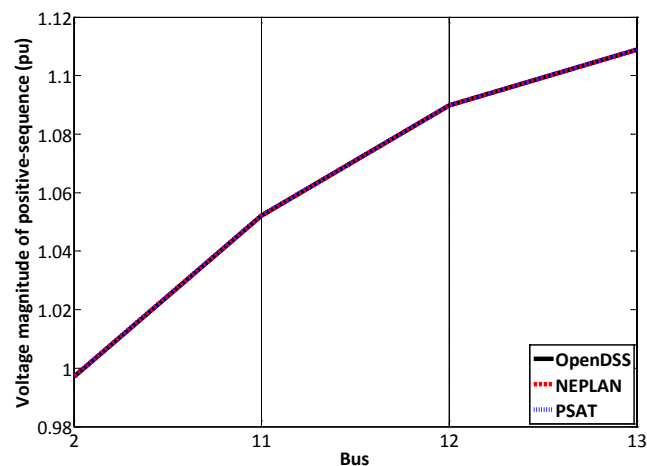


Fig. 3.19: Voltage profile of the third MV feeder

3.4.3. Power flow accuracy check for one of the project pilot installations

The pilot installation of Elektro Gorenjska is shown in Fig. 3.20, consisting of a typical MV/LV distribution transformer, 70 inductive unbalanced loads, and 6 DRESs. The total real and reactive power of all loads is presented in Table 3-7. The rated apparent power of the 6 inverters, as well as the transformer data are shown in Tables 3-8 and 3-9, respectively. Finally, the cross-sections of the 4-wire distribution lines range from 4x16 mm² to 4x150 mm², while their lengths vary from 10 m up to 176 m.

INCREASE – *Increasing the penetration of renewable energy sources in the distribution grid by developing control strategies and using ancillary services*
 D3.1 - Dynamic equivalent models for the simulation of controlled DRES

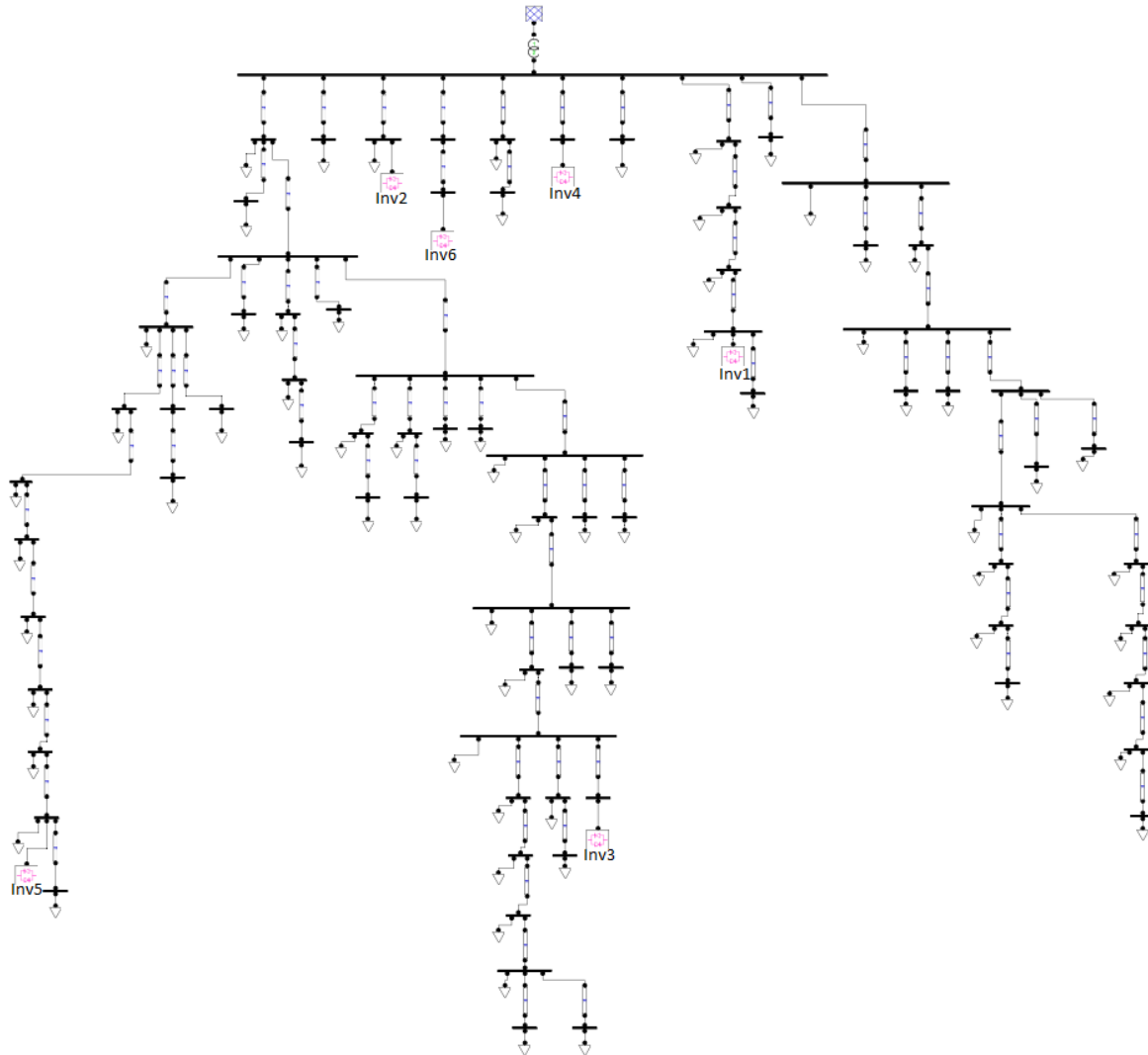


Fig. 3.20: Elektro Gorenjska network topology designed in Draw

Table 3-7: Total unbalanced load

	Real power (kW)	Reactive power (kVAr)
Phase A	58.5	29.25
Phase B	72	37
Phase C	70	35.5

INCREASE – *Increasing the penetration of renewable energy sources in the distribution grid by developing control strategies and using ancillary services*

D3.1 - Dynamic equivalent models for the simulation of controlled DRES

Table 3-8: Inverters rated power

	Rated power (kVA)
Inverter 1	22
Inverter 2	29
Inverter 3	44
Inverter 4	50
Inverter 5	15
Inverter 6	49

Table 3-9: Distribution transformer characteristics

S_n (kVA)	U_n (kV)	Vector group	u_k (%)	No-load losses (W)	On-load losses (W)
250	20 / 0.4	Dyn5	4	425	3250

Table 3-10 presents the relative differences of the phase voltages obtained by OpenDSS and NEPLAN. Assuming NEPLAN as reference, the relative error is smaller than 0.22 % in the presented indicative nodes, while it generally does not exceed 0.5 % in the whole pilot installation.

Table 3-10: Relative differences (%) of power flow results in various nodes

BUS	Phase A	Phase B	Phase C
LV	0.12	0.05	0.10
Inv 1	0.13	0.04	0.08
Inv 2	0.11	0.05	0.10
Inv 3	0.22	0.03	0.01
Inv 4	0.11	0.06	0.09
Inv 5	0.21	0.02	0.05
Inv 6	0.12	0.06	0.09

3.4.4. Numerical accuracy check for extremely unbalanced loads

The high numerical accuracy of the selected OpenDSS platform over other power flow software packages is clearly shown in cases of extremely unbalanced conditions. Such an example is presented in Fig. 3.21, where a simplified MV/LV network is examined, consisting of a MV line and a MV/LV transformer with their characteristics given in Tables 3-11 and 3-12, respectively. An unbalanced constant PQ load is connected to phase C_a with real and reactive power equal to 200 kW and 100 kVAR and the remaining phases are open-ended. In Tables 3-13 and 3-14 the resulting voltages and currents are presented for all nodes and phases, as calculated by both OpenDSS and NEPLAN software. The latter has been selected as a typical representative of commercial power system analysis platforms implementing

INCREASE – Increasing the penetration of renewable energy sources in the distribution grid by developing control strategies and using ancillary services

D3.1 - Dynamic equivalent models for the simulation of controlled DRES

symmetrical components for the calculation of asymmetrical power flow. From the NEPLAN results it is evident that the slack bus is not a stiff power source, while the open-ended phases C_b and C_c also seem to yield small currents. Such numerical errors are introduced by the transformations from phase- to symmetrical-components-domain and vice versa and are totally avoided in the approach adopted by OpenDSS.

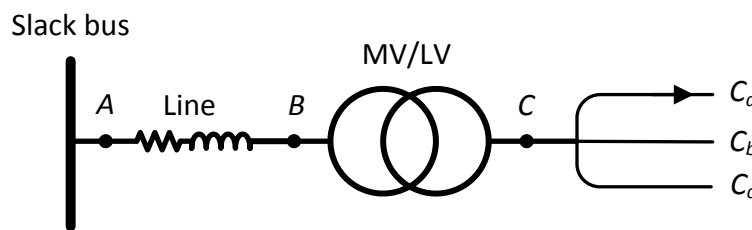


Fig. 3.21: Simplified MV/LV network

Table 3-11: Line characteristics

R_1 (Ω/km)	X_1 (Ω/km)	B_1 (Ω/km)	R_0 (Ω/km)	X_0 (Ω/km)	B_0 (Ω/km)	Length (km)
0.215	0.334	$6.92 \cdot 10^5$	0.363	1.556	$6.92 \cdot 10^5$	1

Table 3-12: Transformer characteristics

S_n (kVA)	U_n (kV)	Vector group	R_1 (pu)	X_1 (pu)	R_0 (pu)	X_0 (pu)
630	20 / 0.4	Dyn5	0.0116	0.119	0.0111	0.114

Table 3-13: Power flow voltage results

Node	Phase a				Phase b				Phase c			
	OpenDSS		NEPLAN		OpenDSS		NEPLAN		OpenDSS		NEPLAN	
	Ampl. (pu)	Angle (deg)										
A	1	0	0.99894	0.01	1	240	1.00066	240.05	1	120	1.00039	119.94
B	0.99958	0	0.99852	0.01	0.99999	240	1.00066	240.05	0.99975	120	1.00015	119.92
C	0.92033	-36.6	0.91998	-36.67	0.99789	210	0.9975	210.08	1.00067	89.9	1.00172	89.87

Table 3-14: Power flow current results

Node	Phase a				Phase b				Phase c			
	OpenDSS		NEPLAN		OpenDSS		NEPLAN		OpenDSS		NEPLAN	
	Ampl. (A)	Angle (deg)										
B	12.1469	-63.21	12.13759	-63.2	0	-	0.01661	-30.01	12.1468	116.79	12.1515	116.85
C	1052	116.79	1052.43	116.77	0	-	0.00417	-48.57	0	-	0.00417	191.43

INCREASE – *Increasing the penetration of renewable energy sources in the distribution grid by developing control strategies and using ancillary services*

D3.1 - Dynamic equivalent models for the simulation of controlled DRES

3.4.5. Numerical performance check in grids with controllable DG units

The performance of the OpenDSS with the presence of controllable DG units is demonstrated in the LV feeder of Fig. 3.22. The line parameters of the examined network are listed in Table 3-15. The network includes three-phase balanced constant PQ loads and DGs with different rated power, as shown in Table 3-16. The transformer data are given in Table 3-17. The slack bus voltage is assumed 1.05 pu (21 kV) to ensure overvoltages higher than 1.06 pu along the network, leading to the activation of the droop control, as shown in Fig. 3.23. In practice, this is often the case as the ratio of the transformer is manually set to avoid undervoltages in high loading conditions without taking into account the increasing penetration of DG units.

The SIMULINK software is used for time domain simulation of the performance of the controlled DGs, since user defined elements cannot be implemented in almost none of the commercially available software packages. Results are compared with the corresponding by the OpenDSS. In Table 3-18 the injected power of each DG unit is presented in the case of no droop control, as well as in the case where droop control is implemented in both OpenDSS and SIMULINK software. Results are in very good agreement with the maximum difference of the injected power being only 6 W, which corresponds to a near-zero mismatch. In Fig. 3.24 the voltage profile along the LV feeder is illustrated, where the activation of droop control mitigates overvoltage. The two curves corresponding to the implementations of droop control in OpenDSS and SIMULINK practically overlap. The superior numerical efficiency of the phasor-domain OpenDSS tool over the time-domain SIMULINK is evident by the fact that the total execution time for OpenDSS is only 100 ms, while the corresponding time for SIMULINK exceeds 1 min.

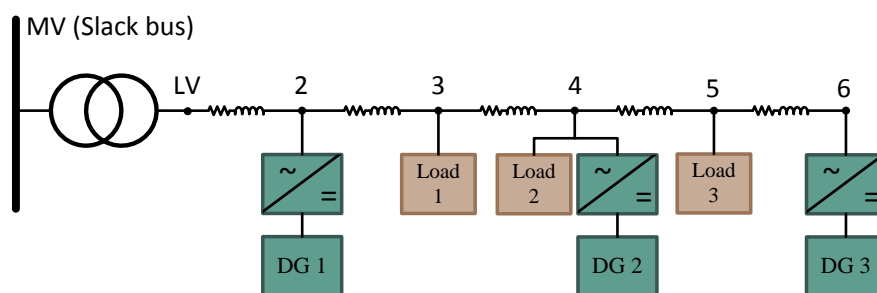


Fig. 3.22: LV feeder with controllable DG units

INCREASE – Increasing the penetration of renewable energy sources in the distribution grid by developing control strategies and using ancillary services

D3.1 - Dynamic equivalent models for the simulation of controlled DRES

Table 3-15: Characteristics of the lines

Line	R_l (Ω/km)	X_l (Ω/km)	C_l (nF/km)	Length (km)
LV-2	0.456	0.088	250	0.057
2 - 3	0.468	0.085	250	0.094
3 - 4	0.48	0.08	250	0.025
4 - 5	0.462	0.083	250	0.132
5 - 6	0.924	0.076	200	0.066

Table 3-16: Generation and consumption units

DGs	Rated real power (kW)	Loads	Real power (kW)	Reactive power (kVAr)
DG 1	20	Load 1	4.5	2.25
DG 2	25	Load 2	3	1.5
DG 3	15	Load 3	6	3

Table 3-17: Characteristics of the transformer

S_n (kVA)	U_n (kV)	Vector group	u_k (%)	No-load losses (W)	On-load losses (W)
250	20 / 0.4	Dyn5	4	325	3250

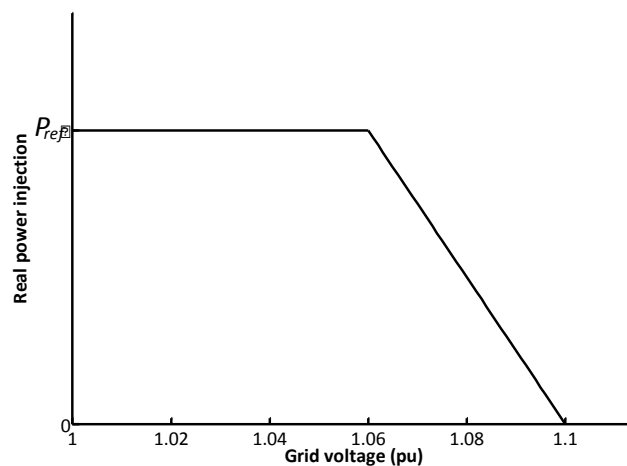


Fig. 3.23: Droop curve of controllable DG unit

Table 3-18: Injected real power of DGs

DGs	P_{inj} (kW)		
	Without droop control	With droop control in OpenDSS	With droop control in SIMULINK
DG 1	20	19.626	19.627
DG 2	25	20.892	20.886
DG 3	15	10.579	10.579

INCREASE – *Increasing the penetration of renewable energy sources in the distribution grid by developing control strategies and using ancillary services*

D3.1 - Dynamic equivalent models for the simulation of controlled DRES

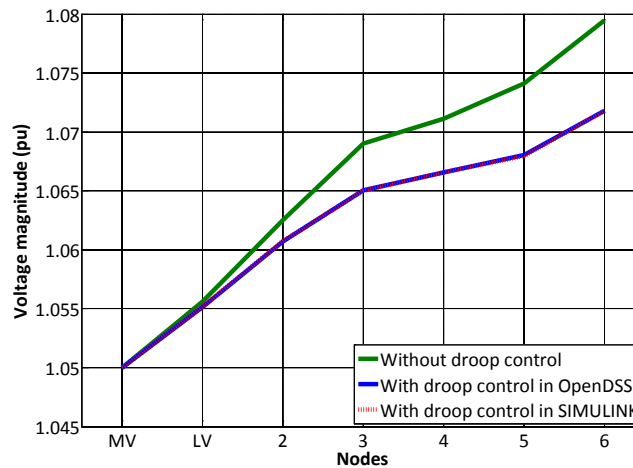


Fig. 3.24: Voltage profile along the LV feeder

4. Implementation of Local Control

4.1. Introduction

Local control is a low-level control applied to controllable DG units via grid-interfaced inverters in order to maintain the stability and the smooth operation of the distribution network. Its distinct advantage is the exclusive use of local parameters, such as voltage at the PCC, which offers the ability to immediately react on grid disturbances.

In the INCREASE simulation platform the local control is implemented from a power systems point of view, neglecting its power electronics origin. Thus, the network is analyzed under quasi-dynamic conditions, ignoring the quick responses of power electronic switching elements like IGBTs. The implemented local control is able to integrate several control schemes of inverter-interfaced controllable DG units. However, in the framework of the INCREASE project, two basic control schemes are incorporated, namely the droop control of the injected real power with respect to grid voltage and the voltage unbalance mitigation.

4.2. Local Control formulation

4.2.1. Droop control

In Deliverable D2.4 it has been adequately justified that in LV grids, where distribution lines have mainly resistive characteristics, efficient voltage control can be accomplished only by controlling the real power output of the DGs connected to the LV grid feeders. Therefore, the principal objective of this control is the real power curtailment of DG units in order to avoid unacceptable voltage rise along the distribution lines where these units are connected. This avoids the turn-off of the DG units due to over-voltages, while the voltage profile of the

distribution feeder is actively controlled. The droop control is based on the voltage at the PCC U_g , while a typical a droop curve is depicted in Fig. 4.1.

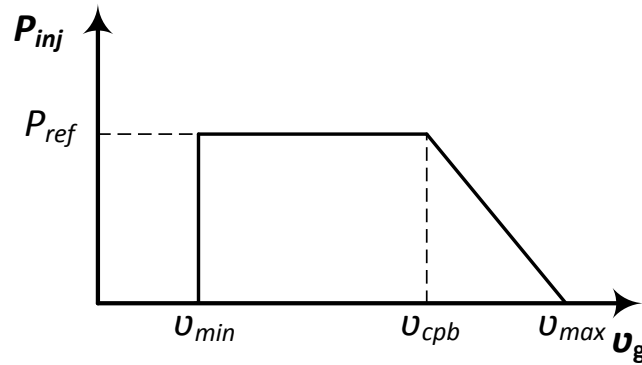


Fig. 4.1: Droop curve of controllable DG units

Voltages U_{cpb} and U_{max} denote the thresholds for the activation of real power curtailment and for the complete cut-off of the power injection, respectively. Additionally, U_{min} is the inverter minimum operating voltage, whereas P_{ref} is the maximum real power the inverter can deliver at a specific time instant, defined from the available power of the primary source. The droop curve is mathematically expressed in (4.1). Assuming asymmetrical operation of the distribution grid, the maximum rms voltage among the three phases is considered for the calculation of the injected real power.

$$P_{inj} = \begin{cases} 0, & \text{if } U_g < U_{min} \\ P_{ref}, & \text{if } U_{min} \leq U_g < U_{cpb} \\ P_{ref} \frac{U_{max} - U_g}{U_{max} - U_{cpb}}, & \text{if } U_{cpb} \leq U_g < U_{max} \\ 0, & \text{if } U_g \geq U_{max} \end{cases} \quad (4.1)$$

4.2.2. Voltage unbalance mitigation

In the second integrated control scheme inverters mitigate voltage unbalance by injecting zero- and negative-sequence currents proportionally to the zero- and negative-sequence voltages at the PCC, respectively. This proportional term is called damping conductance g_d and results in a resistive behaviour of the inverter towards the zero- and negative-sequence components of the grid voltage. The injected currents in symmetrical components are calculated according to

INCREASE – Increasing the penetration of renewable energy sources in the distribution grid by developing control strategies and using ancillary services

D3.1 - Dynamic equivalent models for the simulation of controlled DRES

$$\begin{bmatrix} \underline{i}_0 \\ \underline{i}_1 \\ \underline{i}_2 \end{bmatrix} = \begin{bmatrix} g_d & 0 & 0 \\ 0 & g_1 & 0 \\ 0 & 0 & g_d \end{bmatrix} \cdot \begin{bmatrix} \underline{u}_0 \\ \underline{u}_1 \\ \underline{u}_2 \end{bmatrix} \quad (4.2)$$

where \underline{u}_0 , \underline{u}_1 , \underline{u}_2 are the zero-, positive- and the negative-sequence components of the voltage at the PCC, whereas g_1 refers to the injected real power and is the fundamental conductance of the inverter, having an opposite sign of g_d in case of generation.

The injected phase currents can be easily calculated by applying the inverse transformation from symmetrical-components- to phase-domain. Considering a fixed damping conductance, g_1 is calculated according to

$$g_1 = \frac{3P_{inj}}{\sum |\underline{u}_x|^2 + 2 \sum_{x \neq y} |\underline{u}_x| |\underline{u}_y| \cos(\vartheta_x - \vartheta_y - 2\pi/3)} - \frac{\sum |\underline{u}_x|^2 - \sum_{x \neq y} |\underline{u}_x| |\underline{u}_y| \cos(\vartheta_x - \vartheta_y - 2\pi/3)}{-2g_d \sum |\underline{u}_x|^2 + 2 \sum_{x \neq y} |\underline{u}_x| |\underline{u}_y| \cos(\vartheta_x - \vartheta_y - 2\pi/3)} \quad (4.3)$$

where $|\underline{u}_x|$, $|\underline{u}_y|$ are the magnitudes of phase voltages x , y , while ϑ_x , ϑ_y are the corresponding phase angles. The fundamental conductance is proportional to the injected real power, which is calculated according to the droop curve depicted in Fig. 4.1 and the damping conductance. The reference damping conductance is defined as the ratio of the injected real power (P_{inj}) to the nominal (rated) power of the inverter (P_{nom}) and is calculated in pu according to (4.4). In order to calculate the damping conductance in Siemens (S), (4.4) is multiplied with the Y_{base} derived by the base power and voltage of the inverter.

$$g_d^* = -\frac{P_{inj}}{P_{nom}} \quad (4.4)$$

As analysed in Deliverable D2.4, the implemented Local Control in the INCREASE project considers the damping conductance as a variable parameter depending on the voltage at the PCC. The proposed concept is presented in Fig. 4.2, where on the x axis the maximum of the three phase voltages is considered.

INCREASE – Increasing the penetration of renewable energy sources in the distribution grid by developing control strategies and using ancillary services
D3.1 - Dynamic equivalent models for the simulation of controlled DRES

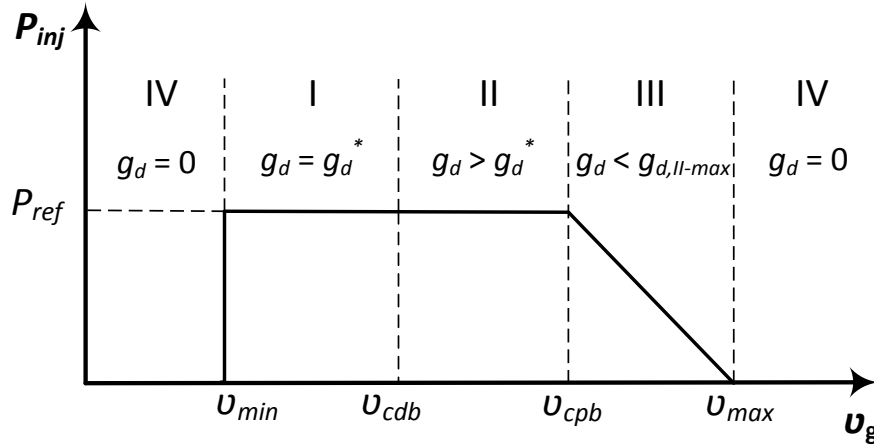


Fig. 4.2: Damping conductance regions

Considering the damping conductance, four regions are introduced: Region I corresponds to the normal operation, where g_d is equal to the reference damping conductance and no real power curtailment occurs. In Region II no power is drooped but the value of g_d is increased, while in Region III the power is drooped and g_d is decreased compared to Region II. Finally, in Region IV the DG unit is disconnected from the grid. The calculation of the damping conductance is expressed in (4.5).

$$g_d = \begin{cases} 0, & \text{if } U_g < U_{min} \\ g_d^* = -\frac{P_{ref}}{P_{nom}}, & \text{if } U_{cdb} \leq U_g < U_{cpb} \\ g_d^* \left(1 + \frac{U_g - U_{cdb}}{U_{cpb} - U_{cdb}} \right) = -\frac{P_{ref}}{P_{nom}} \left(1 + \frac{U_g - U_{cdb}}{U_{cpb} - U_{cdb}} \right), & \text{if } U_{cdb} \leq U_g < U_{cpb} \\ g_d^* \left(1 + \frac{U_g - U_{cdb}}{U_{cpb} - U_{cdb}} \right) = -\frac{P_{ref}}{P_{nom}} \left(\frac{U_g - U_{max}}{U_{max} - U_{cpb}} \right) \left(1 + \frac{U_g - U_{cdb}}{U_{cpb} - U_{cdb}} \right), & \text{if } U_{cpb} \leq U_g < U_{max} \\ 0, & \text{if } U_g \geq U_{max} \end{cases} \quad (4.5)$$

More details of Local Control can be found in the Deliverable D2.4 – ‘Fast control strategy for three phase four wire inverter for DRES’.

4.3. Core and OpenDSS algorithms of Local Control

The integration of the above described Local Control in the INCREASE simulation platform requires the cooperation of three discrete modules, namely Main Routine, Inverter Implementation, and Power Flow Calculation. The first two modules have been developed within the Core of the platform, whereas the third one is provided by the OpenDSS

INCREASE – *Increasing the penetration of renewable energy sources in the distribution grid by developing control strategies and using ancillary services*

D3.1 - Dynamic equivalent models for the simulation of controlled DRES

environment. The aforementioned modules and their respective interactions are illustrated in Fig. 4.3.

- a) Inverter Implementation: This module has been developed to simulate the performance of controllable DG units interfaced to the grid through inverters and is utilized for modeling the developed control schemes for the INCREASE project. It is mainly used for the incorporation of the droop control of the injected real power and of the voltage unbalance mitigation mechanism.
- b) Power Flow Calculation: This module performs the required power flow calculations of asymmetrical networks, where DG units are modeled in each succeeding power flow calculation as constant PQ generators with the ability of injecting (or absorbing) unequal real and reactive power among the phases.
- c) Main Routine: This module is responsible for the activation or termination of Local Control. Moreover, it is the link between the other modules as it receives the set-points regarding the injected complex power of each inverter from the corresponding module and transmits them to OpenDSS via the COM interface. Then, the new voltages derived by the power flow calculation are received from OpenDSS and are forwarded back to the *Inverter Implementation* module so as to define new set-points, etc. This simulation is carried on until a user-defined convergence criterion is satisfied.

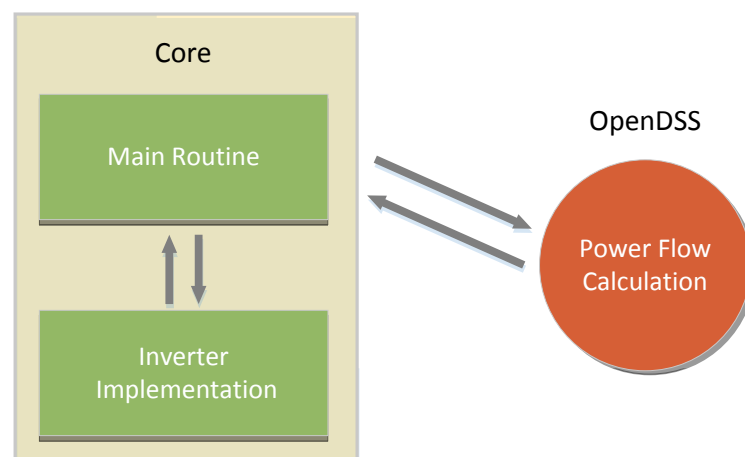


Fig. 4.3: Main components interaction

The simulation process of Local Control can be extended to several time instants. A time instant corresponds to the operating point for a specific time period, where consumption, generation and network characteristics remain constant. The calculation procedure for a given time instant includes successive power flows, taking into account the implemented

INCREASE – *Increasing the penetration of renewable energy sources in the distribution grid by developing control strategies and using ancillary services*
 D3.1 - Dynamic equivalent models for the simulation of controlled DRES

control schemes of the inverters until a new operational state is achieved. The whole procedure involves four steps and is illustrated in Fig. 4.4 by means of a flowchart.

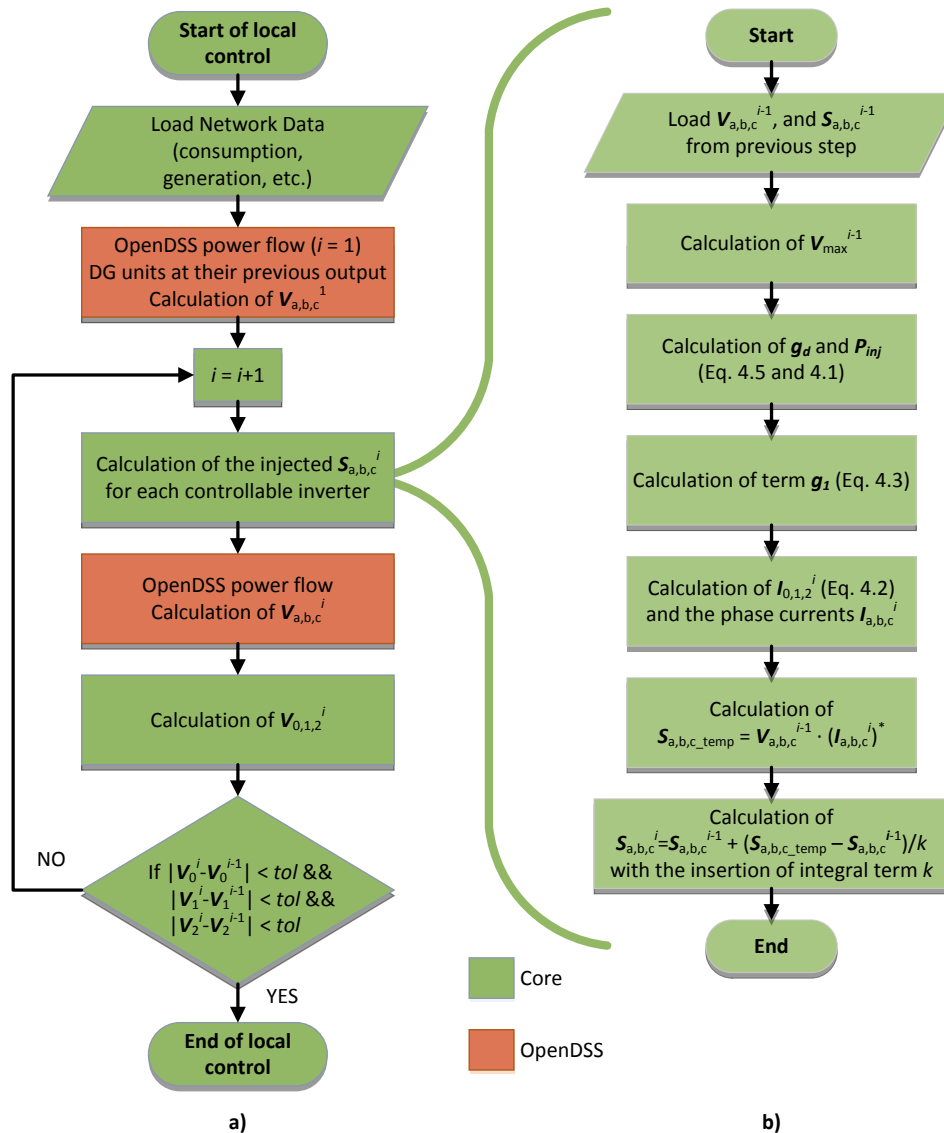


Fig. 4.4: Local Control flowchart: a) Main routine and b) inverter implementation

Step 1: Initial power flow. Initially, the network data regarding loads, generators, inverter new droop curves, etc., are loaded to OpenDSS through the COM interface. Each DG unit injects the real power of the previous time instant and OpenDSS performs a new power flow calculation for the phase-domain voltages at each node.

Step 2: Calculation of the injected complex powers from the DG units. This procedure, depicted in Fig. 4.4b, is implemented in the Core of the INCREASE simulation

INCREASE – *Increasing the penetration of renewable energy sources in the distribution grid by developing control strategies and using ancillary services*

D3.1 - Dynamic equivalent models for the simulation of controlled DRES

platform. First, the vector elements corresponding to the inverter injected complex powers and the relevant voltages of the previous iteration are loaded. Then, the maximum of the three phases voltages is calculated and the injected real power of each inverter, as well as the damping conductance are derived according to the implemented droop control and voltage unbalance mitigation algorithm, respectively. After that, the injected currents in the symmetrical-components- and phase-domain are derived. By multiplying the conjugate phase currents with the respective voltages, a temporary complex power is calculated for each inverter. The final power injection results by taking into consideration the temporary complex power, the injected complex power of the previous iteration step, and a constant integral term k . The scope of this term is further explained Section 4.4.

Step 3: Iterative power flows. Considering the new complex power injections, a new power flow is activated and new phase voltages are calculated.

Step 4: Convergence check. A comparison of voltages in the symmetrical-components-domain at each node between the last and the previous iteration is performed. If the tolerance criterion is satisfied for all nodes, convergence has been achieved and the iterative simulation process terminates. Otherwise, the procedure moves to the next iteration in Step 2.

In the aforementioned simulation procedure it is assumed that the injected real power and the damping conductance are calculated according to the maximum of the three phase voltages. However, the incorporation of Local Control in the INCREASE simulation platform offers the flexibility to examine also different implementations, such as using the positive-sequence voltage for the calculation of the injected real power and the damping conductance. Comparative results concerning different implementations of Local Control are presented in Section 5.

4.4. Numerical performance and accuracy considerations

Considering the simulation procedure, two user-defined tolerance criteria are introduced. The first one refers to the convergence of the power flow calculation by itself in OpenDSS, while the second one is related to the convergence check presented in Step 4 of the simulation procedure, to ensure that the new steady-state conditions have been achieved. The tolerance in Step 4 for the INCREASE simulation platform results shown next has been set to 10^{-3} V.

INCREASE – Increasing the penetration of renewable energy sources in the distribution grid by developing control strategies and using ancillary services

D3.1 - Dynamic equivalent models for the simulation of controlled DRES

In order to avoid spurious numerical oscillations of the injected complex power and grid voltage between two consecutive iterations, the new injected complex power for each inverter $S_{a,b,c}^i$ is calculated taking into account the value of the previous iteration $S_{a,b,c}^{i-1}$ and using an integral term k , defined as

$$S_{a,b,c}^i = S_{a,b,c}^{i-1} + \frac{S_{a,b,c_temp} - S_{a,b,c}^{i-1}}{k} \quad (4.6)$$

where S_{a,b,c_temp} is the injected complex power, resulting from the droop control and the voltage unbalance mitigation scheme, implemented for the corresponding DG.

Numerical oscillations of grid voltage for a sample network are presented in Fig. 4.5 for different values of the integral term k . The value of k can generally vary from small values, which introduce small damping but accelerate convergence, to large values, which lead to slow convergence but to more robust results. A trade-off between convergence rate and damping of oscillations should be made for the right choice of the integral term. It is generally observed that values greater than 2 mitigate the oscillations quite effectively, while a value of $k = 5$ has been used, as default, in the INCREASE simulation platform. It must be noted that different values of k always lead to the same final result and do not influence the accuracy of the results, although they change the numerical performance and stability of the algorithm.

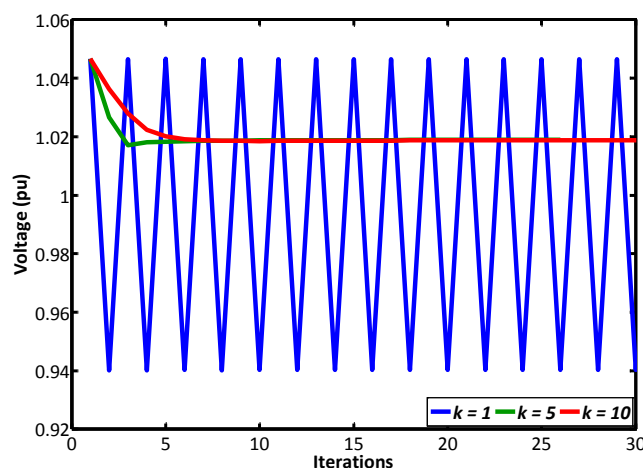


Fig. 4.5: Numerical oscillations on the calculation of grid voltage

INCREASE – *Increasing the penetration of renewable energy sources in the distribution grid by developing control strategies and using ancillary services*

D3.1 - Dynamic equivalent models for the simulation of controlled DRES

5. Simulation results

The Local Control implemented in the INCREASE simulation platform is examined in four different case studies. The first test case consists of a LV feeder with 9 controllable inverters, where the numerical performance of the Local Control scheme is thoroughly investigated. The second test case study is a MV network with 3 radial branches and 5 aggregated DRESs, where the performance of the INCREASE simulation platform is analyzed. Finally, the other 2 test cases are the real pilot installations of Elektro Gorenjska and Stromnetz Steiermark.

In the following simulations 5 different control schemes are assumed and investigated:

1. *Vmax Control*, which is an implementation of the presented Local Control, combining both droop control and unbalance mitigation, using the maximum of the three phase-to-neutral voltages at the PCC for the droop control and the calculation of the damping conductance.
2. *V1 Control*, which is similar to *Vmax Control* approach, but using the positive-sequence of voltage at the PCC instead of the maximum one.
3. *Without Control*, where no control is assumed and DRESs inject their nominal real powers symmetrically to the three phases.
4. *Only Droop*, where the conventional droop control of Section 4.2.1 is only considered.
5. *Only Unbalance*, where the voltage unbalance mitigation algorithm of Section 4.2.2 is only considered.

5.1. Test case 1 – LV network

The examined test case of Fig. 3.14 is considered and presented again in Fig. 5.1. The rated power of the 9 inverters and the total unbalanced load are given in Tables 5-1 and 5-2, respectively. The cross-section of the 4-wire distribution lines ranges from $4 \times 16 \text{ mm}^2$ to $4 \times 70 \text{ mm}^2$ with lengths varying from 10 m up to 100 m, whereas a typical MV/LV distribution transformer is considered with its characteristics given in Table 5-3.

INCREASE – Increasing the penetration of renewable energy sources in the distribution grid by developing control strategies and using ancillary services

D3.1 - Dynamic equivalent models for the simulation of controlled DRES

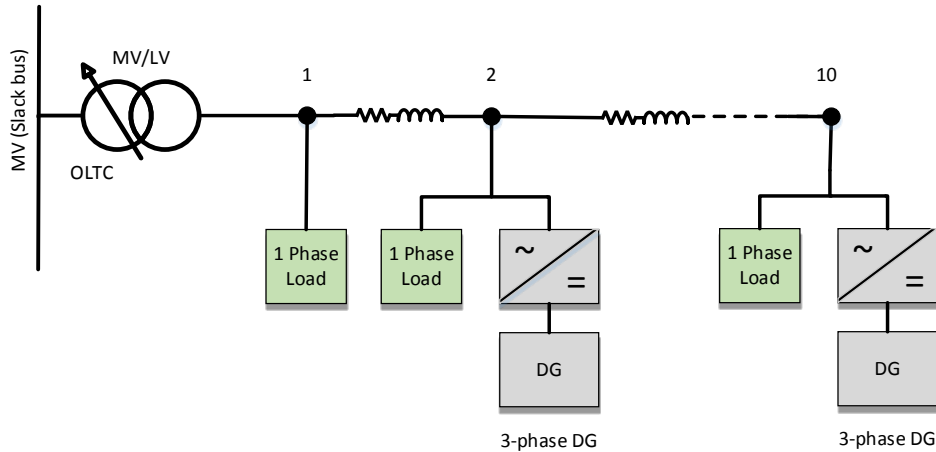


Fig. 5.1: LV network topology

Table 5-1: Inverters rated power

	Rated power (kVA)		Rated power (kVA)
Inverter 1	10	Inverter 6	20
Inverter 2	14	Inverter 7	10
Inverter 3	12	Inverter 8	15
Inverter 4	15	Inverter 9	20
Inverter 5	20		

Table 5-2: Total feeder unbalanced load

	Real power (kW)	Reactive power (kVAr)
Phase A	22.97	7.36
Phase B	10.6	3.45
Phase C	12.8	3.18

Table 5-3: Distribution transformer characteristics

S_n (kVA)	U_n (kV)	Vector group	u_k (%)	No-load losses (W)	Rated load losses (W)
250	20 / 0.4	Dyn5	4	425	3250

5.1.1. Numerical results applying Local Control

A time instant is first considered, assuming the implementation of *Vmax Control* scheme with the slope parameters set to $V_{cdb} = 1.04$ pu, $V_{cpb} = 1.06$ pu, and $V_{max} = 1.1$ pu.

In Fig. 5.2 the convergence of the injected real power of inverter 8 is shown for different values of the integral term k . For k equal to 1 the inverter presents an oscillatory behavior between the droop regions I and IV, thus the network cannot converge to equilibrium. An

INCREASE – *Increasing the penetration of renewable energy sources in the distribution grid by developing control strategies and using ancillary services*
 D3.1 - Dynamic equivalent models for the simulation of controlled DRES

increase of the integral term results in a slower but more robust convergence of inverter real power to its final value. It is noted that the final output of inverter is irrelevant to the value of integral term k , as described previously, validating the proposed Local Control implementation. In Fig. 5.3 a detail of the injected real power is shown for $k = 5$, revealing the convergence rate to the final value between iterations. A total of 16 iterations were needed for convergence according to the predefined tolerance of 10^{-3} V.

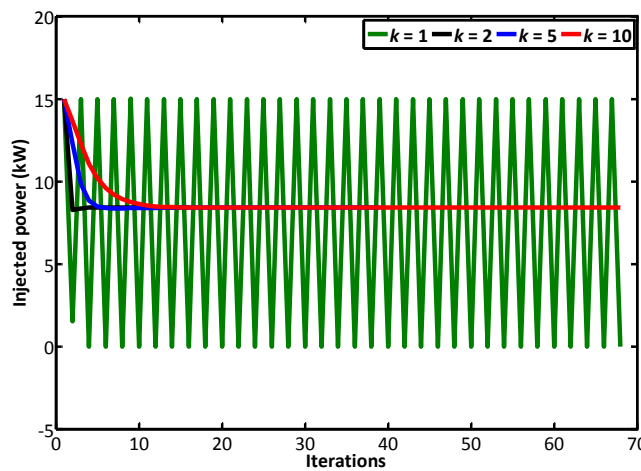


Fig. 5.2: Injected real power of inverter 8

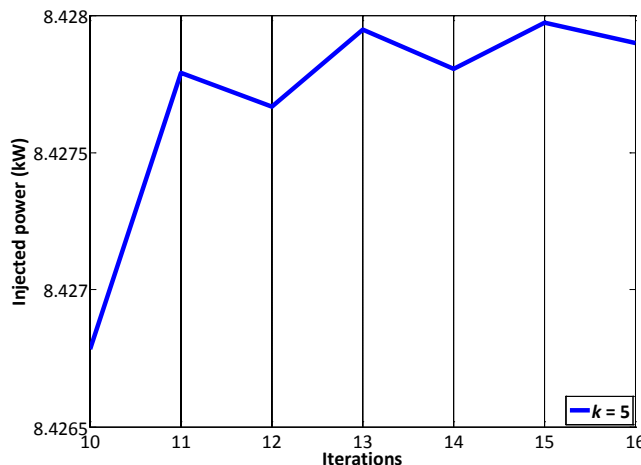


Fig. 5.3: Detail of convergence rate for inverter 8

In Fig. 5.4 the injected real power of all inverters is plotted against the number of iterations. From their final values in 16th iteration it is concluded that the first 4 inverters inject their nominal power, while the remaining inverters are drooped. This happens due to the increased voltage along the feeder, as shown in the voltage profile of the three phase voltages in Fig. 5.5 after the execution of Local Control. An overvoltage above V_{cpb} leads to

INCREASE – Increasing the penetration of renewable energy sources in the distribution grid by developing control strategies and using ancillary services
 D3.1 - Dynamic equivalent models for the simulation of controlled DRES

curtailment in the power output of the DRESs. The resulting power curtailment is not uniform, since the DRESs which are close to the busbars where overvoltage occurs are curtailed more. This unfair situation is subjected to the Overlay Control, which will be presented in the Deliverable D3.2 – ‘Integrated simulation platform which models the key components and control strategies’.

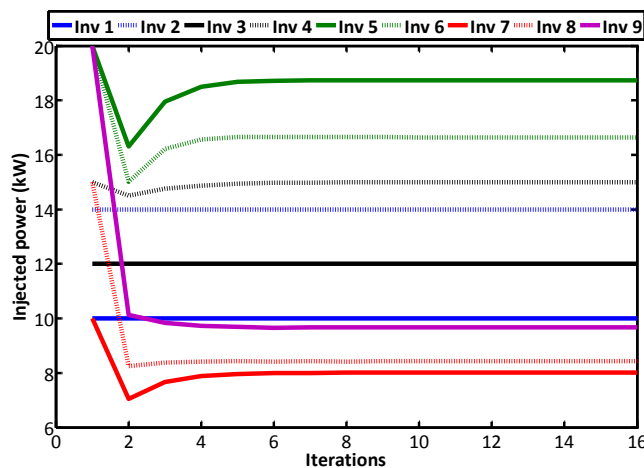


Fig. 5.4: Injected real power of inverters

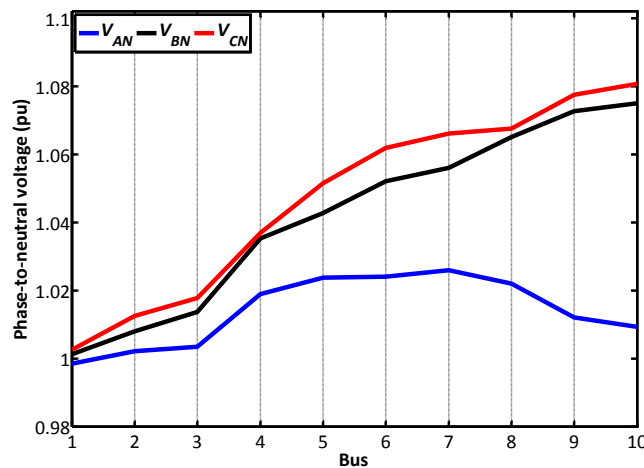


Fig. 5.5: Voltage profile along the LV feeder

5.1.2. Investigation of different local control schemes

Next, for the same network configuration, the *Vmax Control* is compared with the *V1 Control* implementation of Local Control as well as with the other conventional control schemes.

In Fig. 5.6 the total injected power from the DRESs is presented for the examined control techniques. It is evident that the *Without Control* and *Only Unbalance* schemes inject the

INCREASE – Increasing the penetration of renewable energy sources in the distribution grid by developing control strategies and using ancillary services

D3.1 - Dynamic equivalent models for the simulation of controlled DRES

total sum of all inverters rated power, since in these cases the power output of the corresponding DRESs is not curtailed. On the contrary, the curtailment in *Only Droop* scheme is quite significant, due to the droop control that is enabled in most inverters along the LV feeder. The two implementations of Local Control curtail less than the *Only Droop* technique, mainly due to the voltage unbalance mitigation algorithm that is simultaneously performed with the droop control algorithm. Moreover, the *V1 Control* always curtail less than the *Vmax Control*, since the positive-sequence of voltage used in droop control is always smaller (or equal) than the maximum voltage of the three phases.

Furthermore, the power losses of the examined LV feeder along with the transformer are presented in Fig. 5.7 for the different control schemes. It is evident that the losses follow the pattern of the total injected power in Fig. 5.6. This happens since the examined LV feeder presents a reverse flow of real power in all cases, thus the losses along the LV lines and the transformer are proportional to the square of the total injected power from the DRESs.

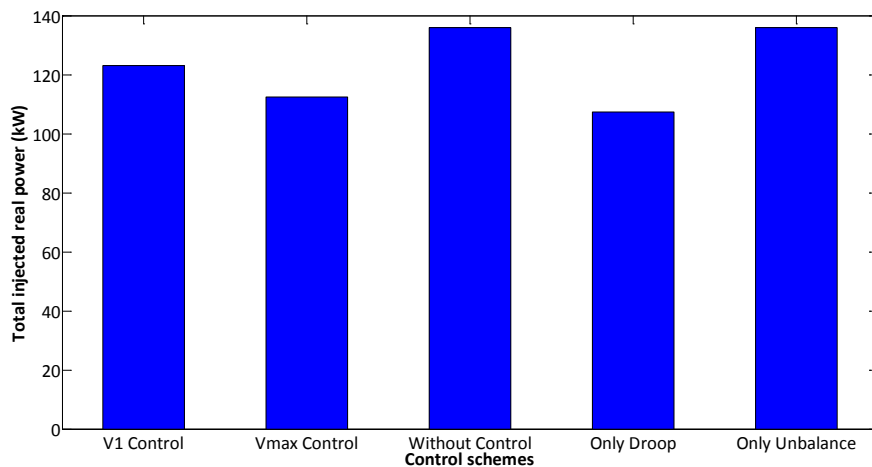


Fig. 5.6: Total inverter injected power for different control schemes

INCREASE – Increasing the penetration of renewable energy sources in the distribution grid by developing control strategies and using ancillary services
 D3.1 - Dynamic equivalent models for the simulation of controlled DRES

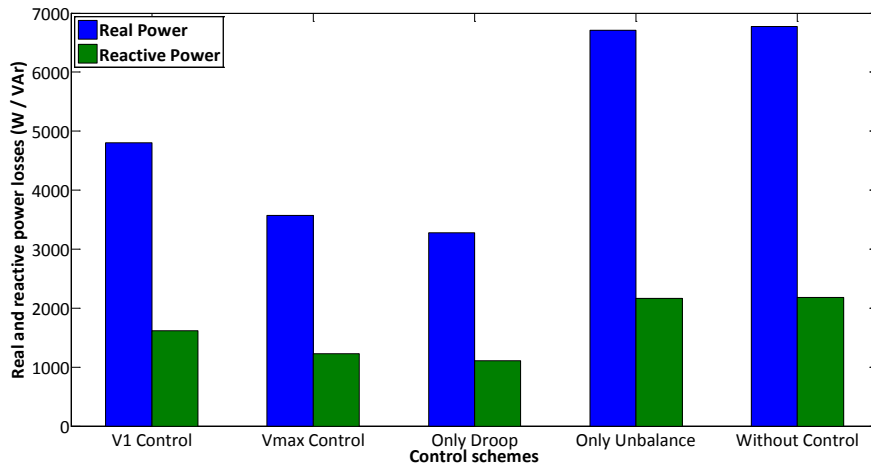


Fig. 5.7: Total power losses for different control schemes

Considering the bus voltages, the voltage profile of phase A and positive-sequence along the LV feeder are presented in Figs. 5.8 and 5.9, respectively. The *Only Droop* control scheme results in the lowest voltage profile, due to the highest curtailment in the total injected power. The *Only Unbalance* technique presents the highest levels of phase-domain voltage, since only the unbalance voltage mitigation algorithm is used, while the positive-sequence voltage is not altered, thus yielding the same levels with the *Without Control* technique. Results of both Local Control versions are between the two other control techniques, with the *Vmax Control* generally leading to lower voltage levels than the *V1 Control*.

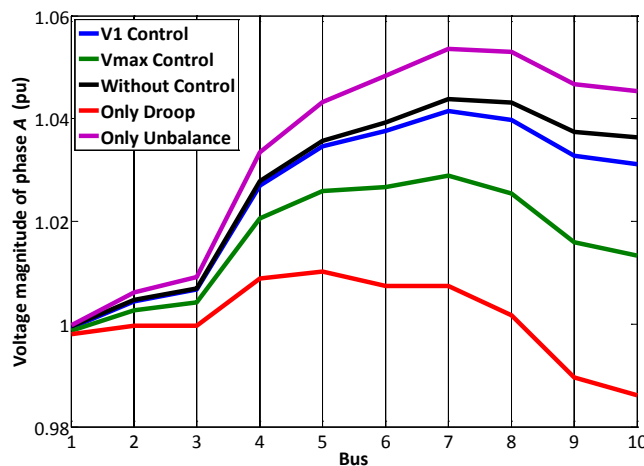


Fig. 5.8: Voltage profile of phase A for different control schemes

INCREASE – Increasing the penetration of renewable energy sources in the distribution grid by developing control strategies and using ancillary services

D3.1 - Dynamic equivalent models for the simulation of controlled DRES

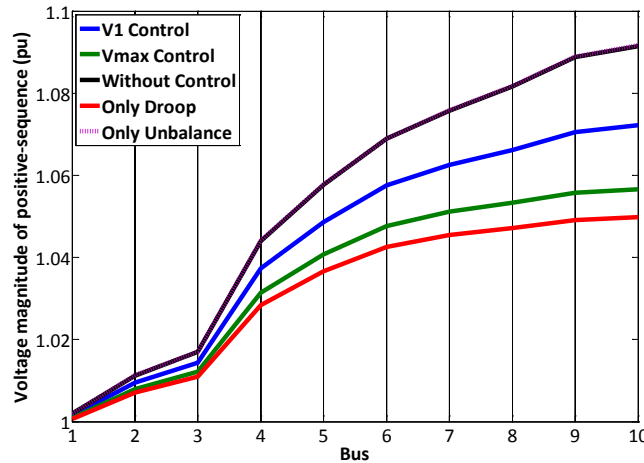


Fig. 5.9: Voltage profile of positive-sequence for different control schemes

The voltage unbalance factors (VUFs) of the zero- and negative-sequence are defined

$$VUF_0(\%) = \frac{V_0}{V_1} 100\% \quad (5.1)$$

$$VUF_2(\%) = \frac{V_2}{V_1} 100\% \quad (5.2)$$

where V_0, V_1 , and V_2 are the zero-, positive-, and negative-sequence of voltage. The VUFs along the feeder are presented in Figs. 5.10 and 5.11, respectively. The *Without Control* and the *Only Droop* control lead to the highest VUF_0 , whereas the remaining control techniques significantly reduce it. This happens due to the voltage unbalance mitigation algorithm that is incorporated in the *Only Unbalance* and in both versions of Local Control. Due to the inclusion of droop control, the VUF_2 generally seem to be increased compared to the results of the *Without Control*. However, this increase is adequately compensated from the voltage unbalance mitigation algorithm, as it is observed when compared with the *Only Droop* technique.

INCREASE – *Increasing the penetration of renewable energy sources in the distribution grid by developing control strategies and using ancillary services*
 D3.1 - Dynamic equivalent models for the simulation of controlled DRES

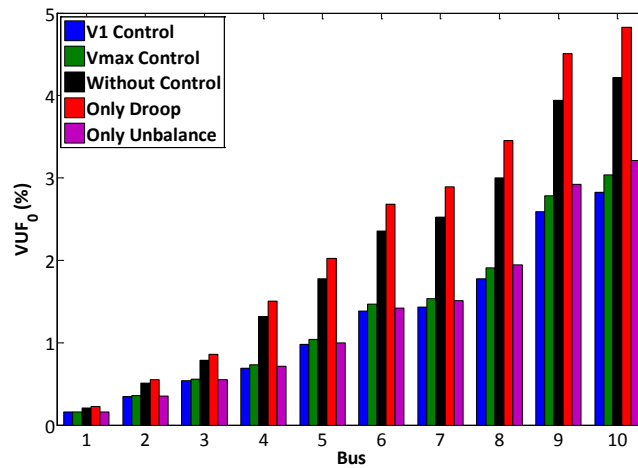


Fig. 5.10: Voltage unbalance factor of zero-sequence along the LV feeder

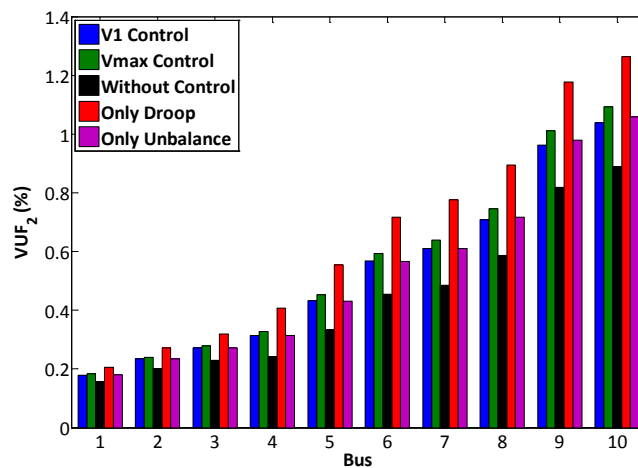


Fig. 5.11: Voltage unbalance factor of negative-sequence along the LV feeder

5.2. Test case 2 – MV network

The examined MV network of Fig. 3.16 is examined, which is presented again in Fig. 5.12. In Table 5-4 the aggregated rated apparent power of the 5 controllable DG units is presented, connected along the MV feeders as shown in Fig. 5.12. In Table 5-5 the aggregated loads of all buses are given, which are assumed balanced between phases due to their direct connection to the MV branches. A typical HV/MV transformer is also considered with its characteristics given in Table 5-6.

INCREASE – Increasing the penetration of renewable energy sources in the distribution grid by developing control strategies and using ancillary services

D3.1 - Dynamic equivalent models for the simulation of controlled DRES

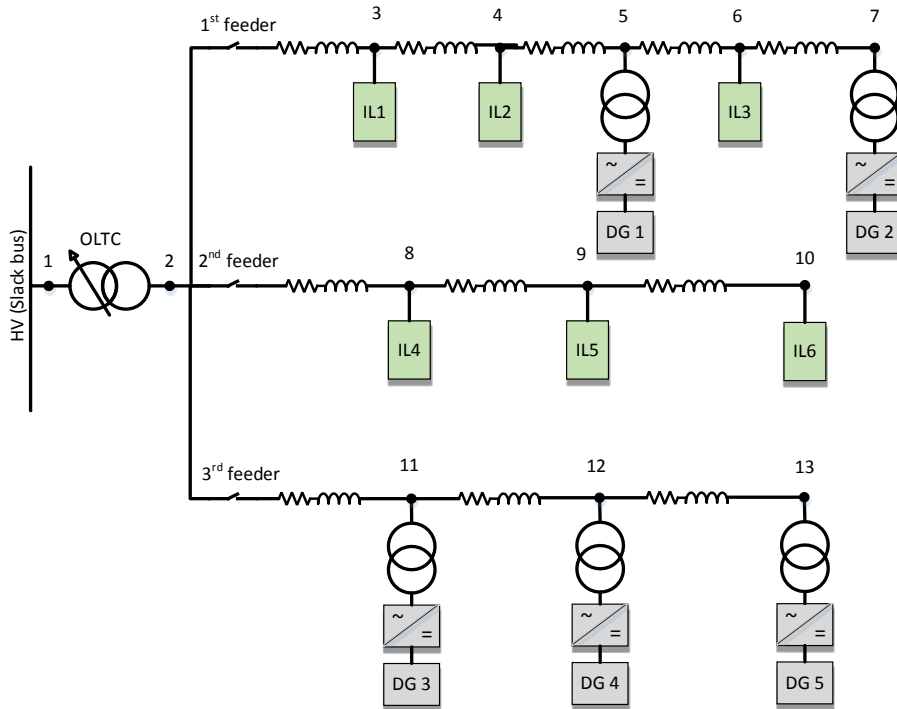


Fig. 5.12: MV network topology

Table 5-4: DG rated powers

	Rated Power (kVA)
DG 1	3500
DG 2	3500
DG 3	3300
DG 4	3300
DG 5	3300

Table 5-5: Aggregated loads

	Real Power (kW)	Reactive Power (kVAr)
Bus 3	2330	1160
Bus 4	2330	1160
Bus 6	2330	1160
Bus 8	1400	700
Bus 9	1400	700
Bus 10	1400	700

Table 5-6: Distribution transformer characteristics

S_n (MVA)	U_n (kV)	Vector group	u_k (%)	No-load losses (kW)	On-load losses (kW)
-------------	------------	--------------	-----------	---------------------	---------------------

INCREASE – Increasing the penetration of renewable energy sources in the distribution grid by developing control strategies and using ancillary services

D3.1 - Dynamic equivalent models for the simulation of controlled DRES

50	150/ 20	Yd5	17.74	165	1250
----	---------	-----	-------	-----	------

5.2.1. Numerical Results applying Local Control

Similar to the previous test case, a time instant is considered, assuming the implementation of *Vmax Control* scheme with the slope parameters set to $V_{cdb} = 1.04$ pu, $V_{cpb} = 1.06$ pu, and $V_{max} = 1.1$ pu. The voltage profile along each MV feeder is presented in Figs. 5.13-5.15. It is evident that it decreases along the second feeder and increases along the third one, due to the exclusive connection of loads and controllable DG units, respectively. The DGs connected to Buses 12 and 13 are drooped and their final injected power is equal to 2.53 and 1.72 MW, respectively. The remaining DG units inject their nominal power since the voltage at their PCC is calculated below V_{cpb} .

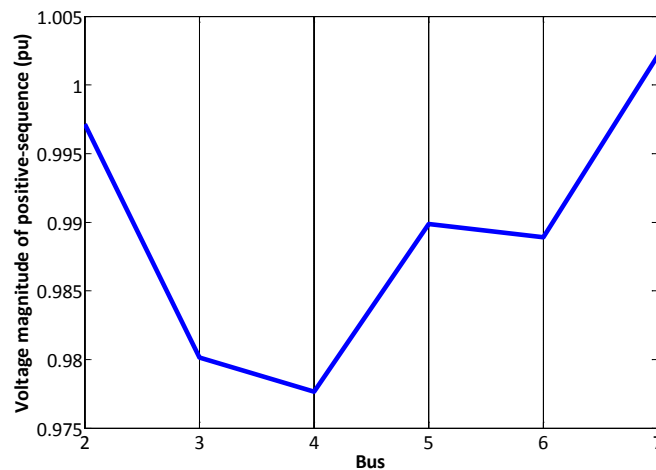


Fig. 5.13: Voltage profile of the first MV feeder

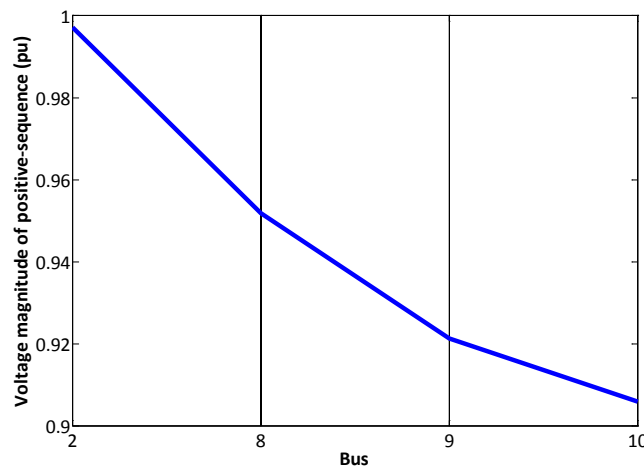


Fig. 5.14: Voltage profile of the second MV feeder

INCREASE – *Increasing the penetration of renewable energy sources in the distribution grid by developing control strategies and using ancillary services*

D3.1 - Dynamic equivalent models for the simulation of controlled DRES

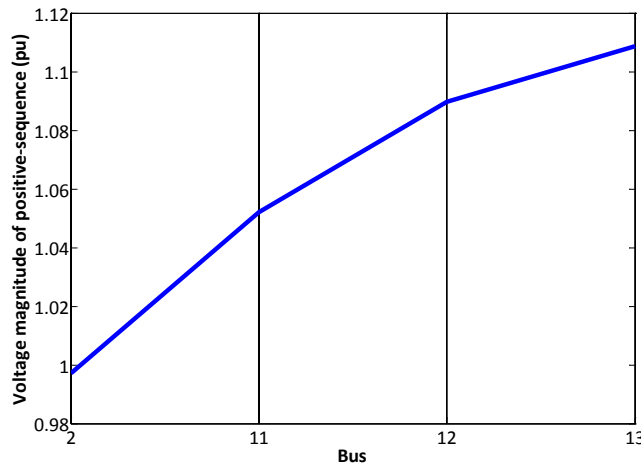


Fig. 5.15: Voltage profile of the third MV feeder

5.2.2. Investigation of different control schemes

The *Vmax Control* is compared with the *V1 Control* implementation of Local Control as well as with the other conventional control schemes. The *Only Unbalance* technique is excluded from this analysis, since all loads are considered fully balanced in the three phases, a typical situation for most MV grids.

In Fig. 5.16 the total injected power from the DG units is illustrated for the presented control techniques. It is evident that the *Without Control* scheme injects the total sum of all inverter rated powers, since the output of the corresponding DG units is not curtailed. The curtailment in *Only Droop* scheme is quite significant, due to the droop control that is enabled in most inverters along the MV feeders. Furthermore, due to the absence of voltage unbalance in MV networks, the positive-sequence voltage is almost identical to the maximum phase voltage, thus the two implementations of Local Control curtail the same amount of power with the *Only Droop* technique.

Additionally, the power losses of the examined MV network and transformer are depicted in Fig. 5.17 for the examined control schemes. It is clear that the losses follow the pattern of the total injected power of Fig. 5.6, since the active power curtailment occurs only at the third feeder of the MV network where a reverse flow of real power is observed. Therefore, the network losses are proportional to the square of the total injected power from the DG units.

INCREASE – Increasing the penetration of renewable energy sources in the distribution grid by developing control strategies and using ancillary services

D3.1 - Dynamic equivalent models for the simulation of controlled DRES

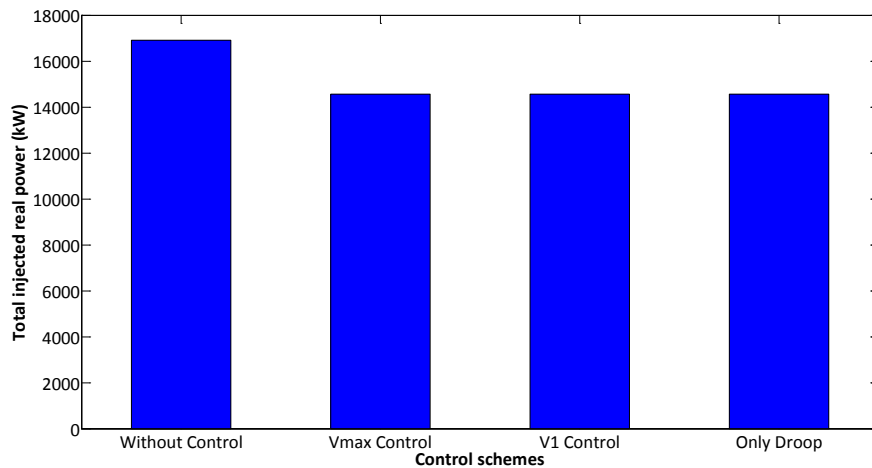


Fig. 5.16: Total inverter injected power for different control schemes

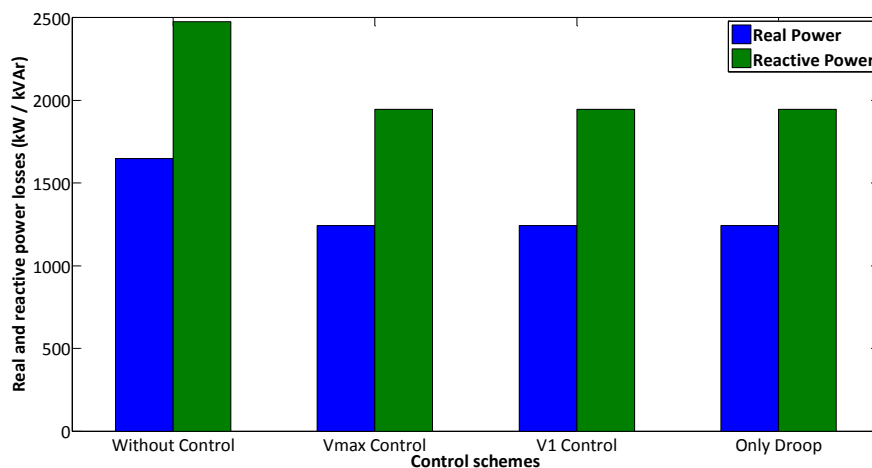


Fig. 5.17: Total power losses for different control schemes

The positive-sequence voltage profile along each feeder is presented in Figs. 5.18-5.20. Since the active power curtailment occurs at the third feeder, the voltage profiles of the other feeders are not affected by the assumed control scheme. Thus, considering the third feeder depicted in Fig. 5.20, the *Only Droop* control technique leads to the lowest voltage profile due to the highest curtailment in the total injected power. Results of both Local Control versions are again identical to the *Only Droop* due to the absence of voltage unbalance control.

INCREASE – Increasing the penetration of renewable energy sources in the distribution grid by developing control strategies and using ancillary services
 D3.1 - Dynamic equivalent models for the simulation of controlled DRES

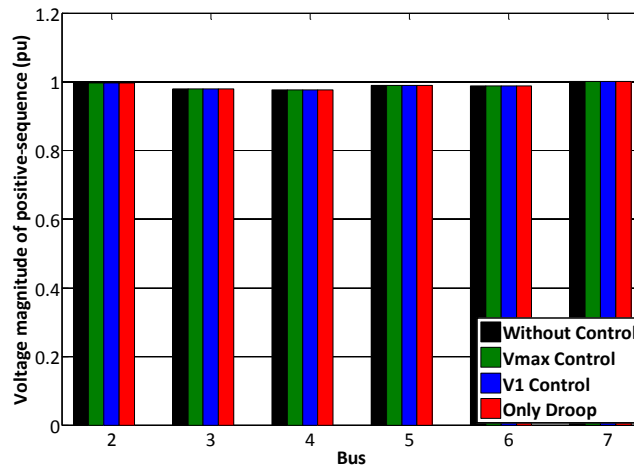


Fig. 5.18: Positive-sequence voltage profile of first MV feeder

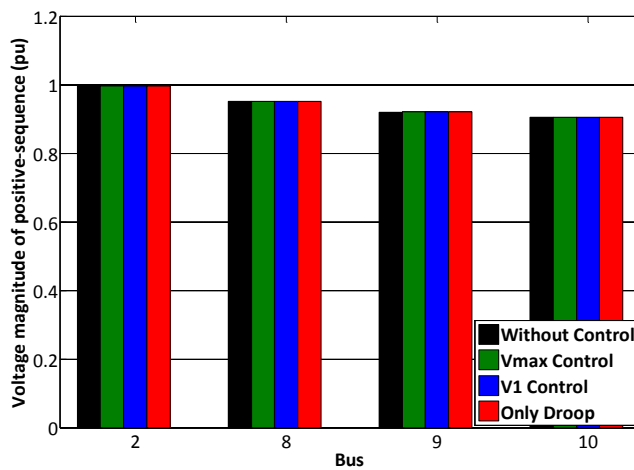


Fig. 5.19: Positive-sequence voltage profile of second MV feeder

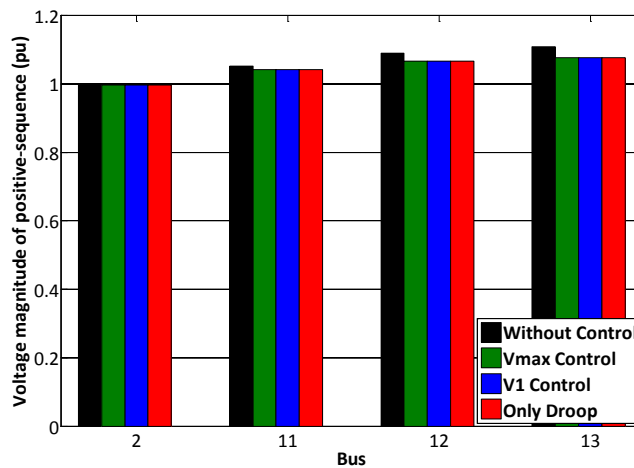


Fig. 5.20: Positive-sequence voltage profile of third MV feeder

5.3. Test case 3 – Elektro Gorenjska pilot installation

In this section, the proposed Local Control is demonstrated in the real pilot installation of Elektro Gorenjska (Fig. 3.20). The examined LV network is shown in Fig. 5.21 and consists of a typical MV/LV distribution transformer, 70 inductive unbalanced time series loads which change every five minutes, and 6 controllable DRESs.

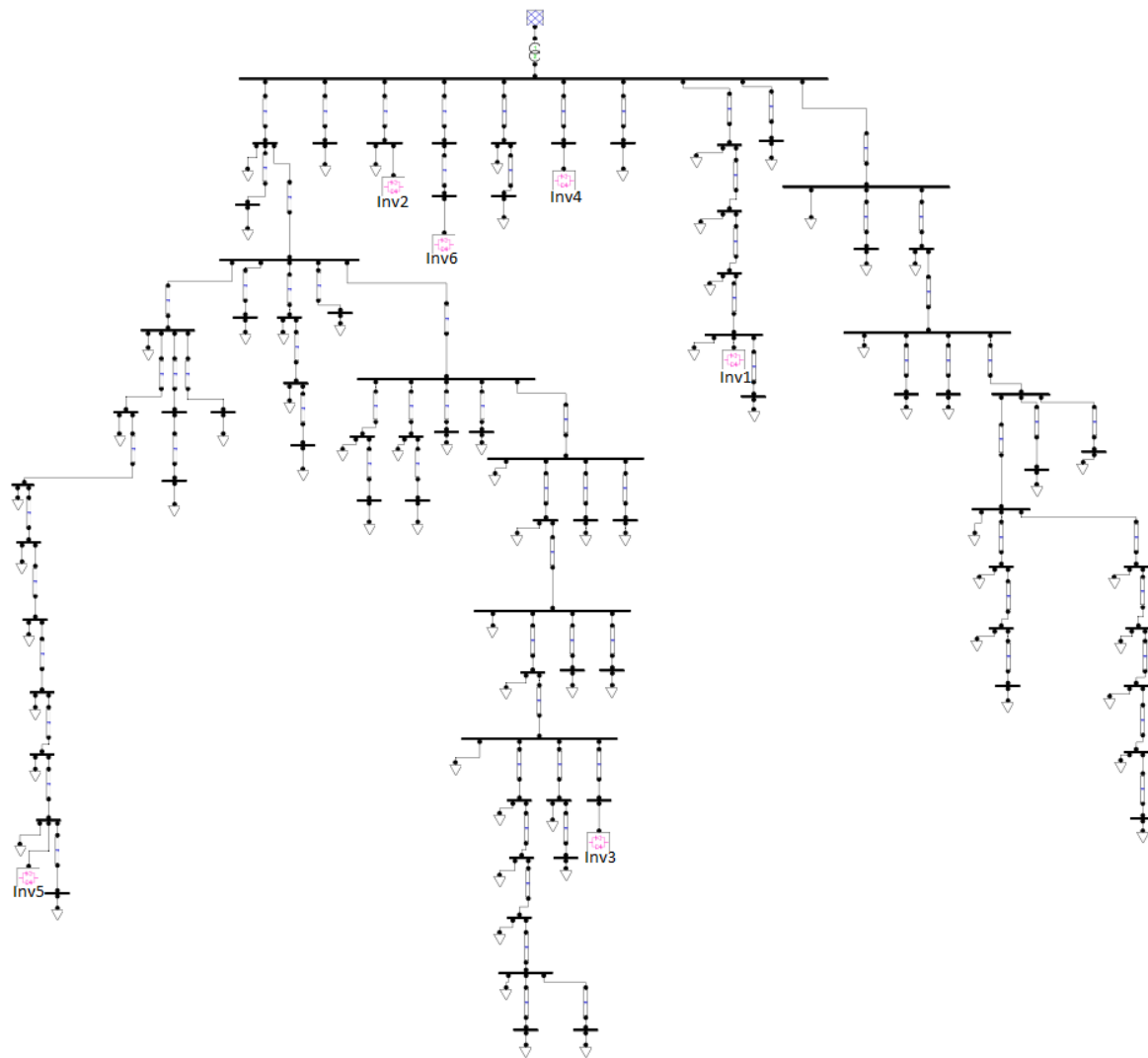


Fig. 5.21: Elektro Gorenjska network topology designed in Draw

The total real and reactive power of all loads is presented in Figs. 5.22 and 5.23, respectively. The rated apparent power of the 6 inverters, as well as the transformer data are shown in Tables 5-7 and 5-8, respectively. Finally, the cross-sections of the 4-wire distribution lines range from $4 \times 16 \text{ mm}^2$ to $4 \times 150 \text{ mm}^2$ with their lengths varying from 10 m up to 176 m.

INCREASE – Increasing the penetration of renewable energy sources in the distribution grid by developing control strategies and using ancillary services

D3.1 - Dynamic equivalent models for the simulation of controlled DRES

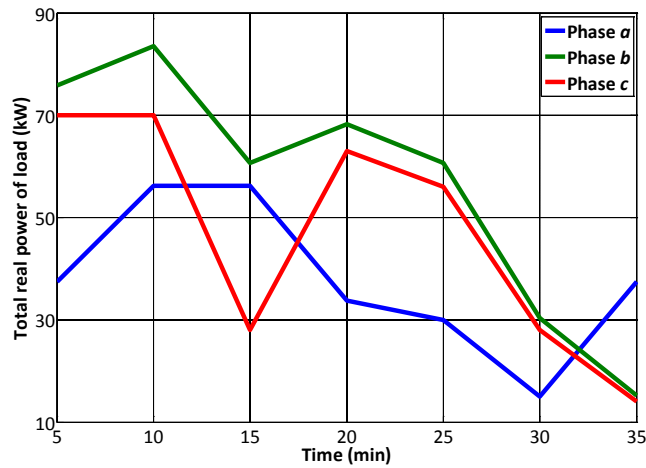


Fig. 5.22: Total real load power

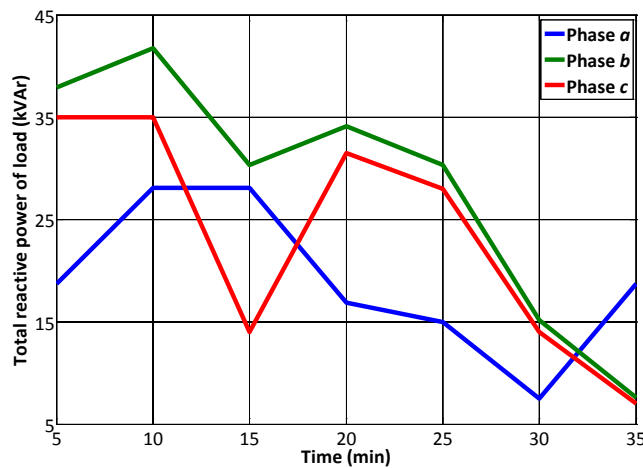


Fig. 5.23: Total reactive load power

Table 5-7: Inverters rated power

	Rated power (kVA)
Inverter 1	22
Inverter 2	29
Inverter 3	44
Inverter 4	50
Inverter 5	15
Inverter 6	49

Table 5-8: Distribution transformer characteristics

S_n (kVA)	U_n (kV)	Vector group	u_k (%)	No-load losses (W)	On-load losses (W)
250	20 / 0.4	Dyn5	4	425	3250

INCREASE – Increasing the penetration of renewable energy sources in the distribution grid by developing control strategies and using ancillary services
 D3.1 - Dynamic equivalent models for the simulation of controlled DRES

5.3.1. Numerical Results applying Local Control

Once again, the slope parameters for the implementation of the *Vmax Control* scheme are set to $V_{cdb} = 1.04$ pu, $V_{cpb} = 1.06$ pu, and $V_{max} = 1.1$ pu. In Fig. 5.24 the injected real power of all inverters is plotted against time. It is obvious that inverter 2 injects constantly their nominal power, whereas the remaining inverters are generally drooped at the different time instants. The corresponding voltages at the PCCs of all inverters are presented in Figs. 5.25-5.27.

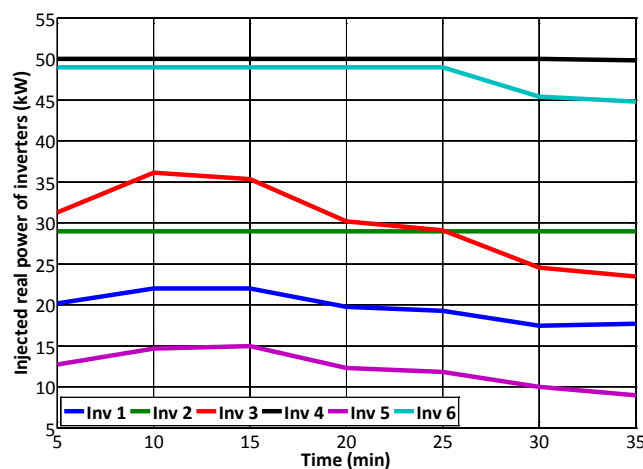


Fig. 5.24: Injected real power of the inverters vs time

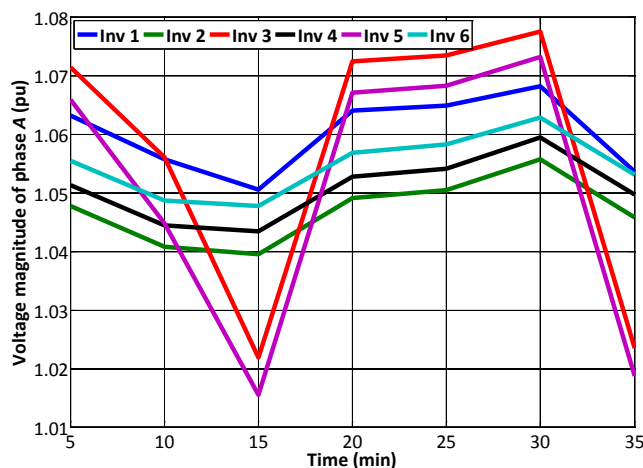


Fig. 5.25: Voltage of phase A for all inverters vs time

INCREASE – Increasing the penetration of renewable energy sources in the distribution grid by developing control strategies and using ancillary services
 D3.1 - Dynamic equivalent models for the simulation of controlled DRES

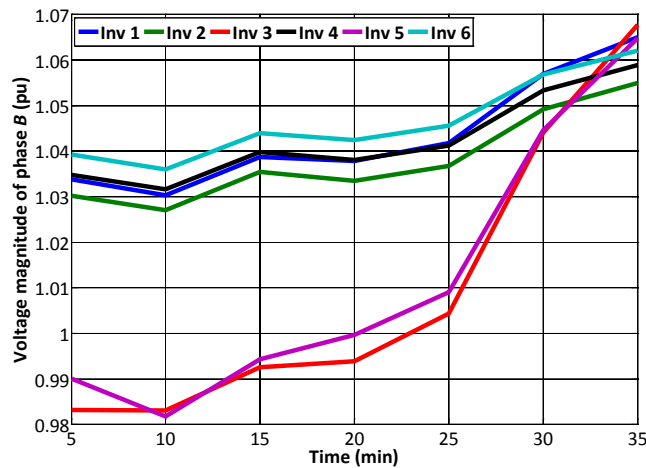


Fig. 5.26: Voltage of phase B for all inverters vs time

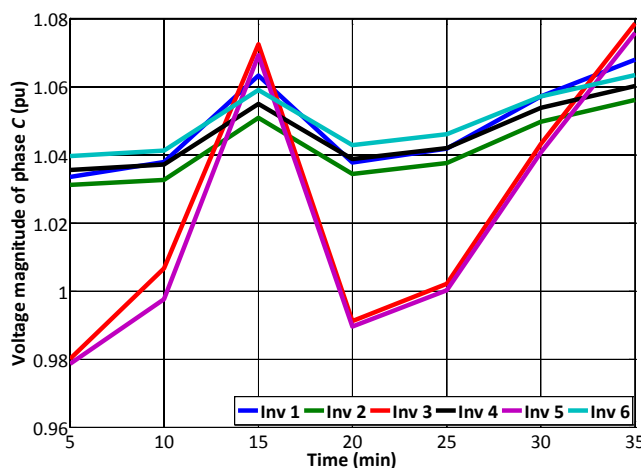


Fig. 5.27: Voltage of phase C for all inverters vs time

5.3.2. Investigation of different control schemes

In this section, the *Vmax Control* is further investigated and compared to the *V1 Control* implementation as well as with the *Only Droop* and *Only Unbalance* control techniques. The positive-sequence voltage and the voltage of phase B, as well as the voltage unbalance factors of zero- and negative-sequence for inverter 3 are presented in Figs. 5.28-5.31. Similar results are also observed for the remaining inverters, thus they are not presented.

Simulations indicate that the *Only Unbalance* control manages to remarkably reduce both VUFs. However, it should not be considered as the most suitable control method, since it is not able by itself to reduce efficiently potential overvoltages. On the other hand, both *V1 Control* and *Vmax Control* have the ability to mitigate properly the examined voltage

INCREASE – Increasing the penetration of renewable energy sources in the distribution grid by developing control strategies and using ancillary services
 D3.1 - Dynamic equivalent models for the simulation of controlled DRES

risers. It should be emphasized again that using the maximum phase voltage seems to be more effective than using the positive sequence voltage.

Moreover, as shown in Figs. 5.30 and 5.31, both Local Control schemes manage to preserve low VUFs levels. The *Only Droop* control scheme seems to be the most efficient solution regarding overvoltage mitigation, since it is able to reduce remarkably the positive-sequence voltage as well as the phase-to-neutral voltages. However, it should be stressed out that this technique considerably deteriorates both VUFs.

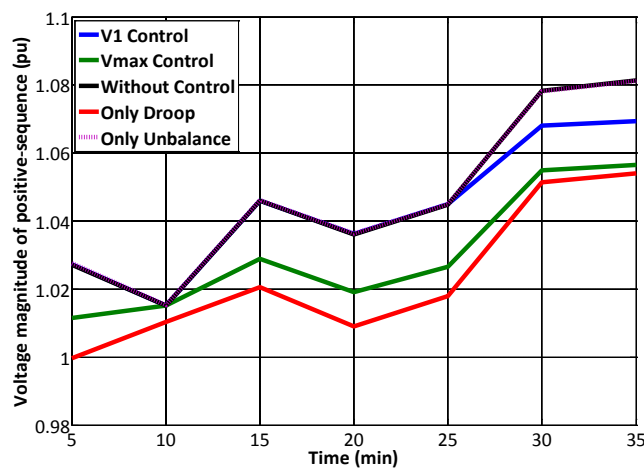


Fig. 5.28: Positive-sequence voltage for inverter 3 vs time

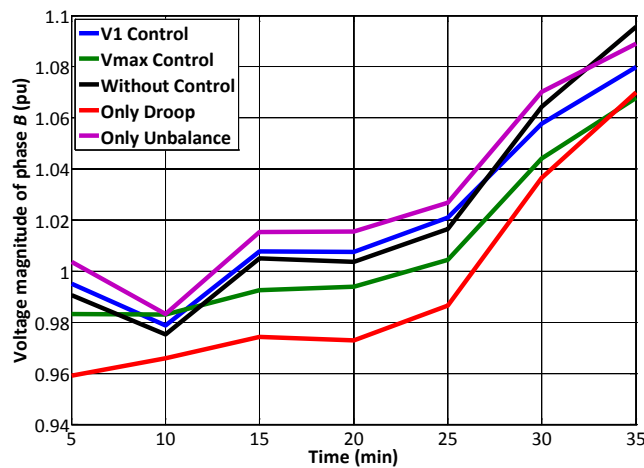


Fig. 5.29: Voltage of phase B for inverter 3 vs time

INCREASE – Increasing the penetration of renewable energy sources in the distribution grid by developing control strategies and using ancillary services
 D3.1 - Dynamic equivalent models for the simulation of controlled DRES

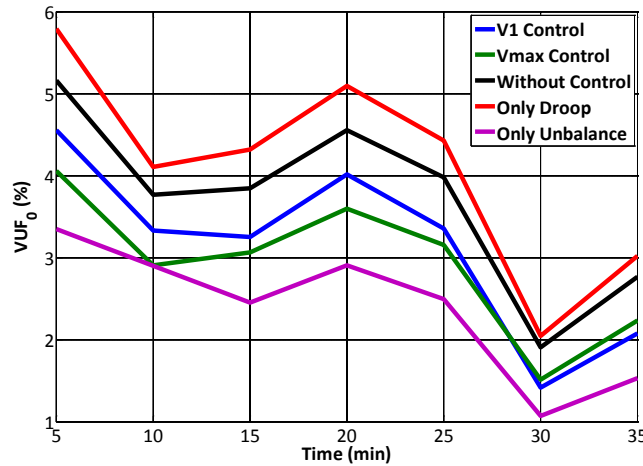


Fig. 5.30: Voltage unbalance factor of zero-sequence for inverter 3 vs time

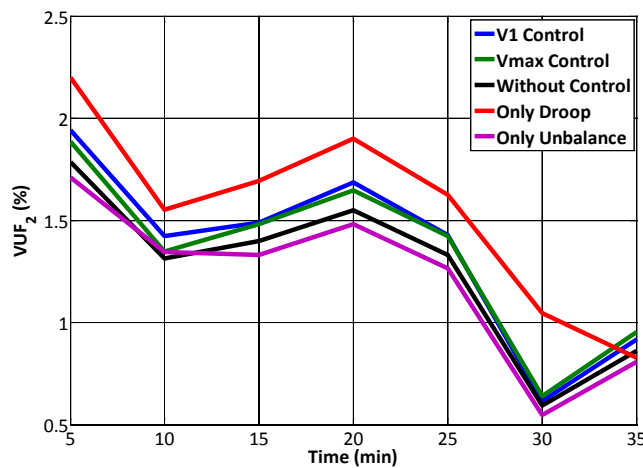


Fig. 5.31: Voltage unbalance factor of negative-sequence for inverter 3 vs time

Finally, in order to assess the proposed implementations of the Local Control, the total power generation is calculated in Fig. 5.32 for each control scheme. In the *Only Unbalance*, as well as in the *Without Control* scheme, the output of the inverters is not curtailed. Thus, the total real power generation is constantly equal to 209 kW, corresponding to the total sum of all inverters rated power. On the other hand, the *Only Droop* technique curtails the total injected power in all time instants, since the droop control is constantly enabled.

In the *Vmax Control* as well as in the *V1 Control* schemes, the droop control technique is applied simultaneously with the voltage unbalance mitigation algorithm. As a result, these control strategies are able to mitigate properly any voltage rises, providing also high penetration levels of DRESs. Once again, it is observed that the *V1 Control* curtails less power

INCREASE – Increasing the penetration of renewable energy sources in the distribution grid by developing control strategies and using ancillary services
 D3.1 - Dynamic equivalent models for the simulation of controlled DRES

than the *Vmax Control*, since the criterion of the positive-sequence voltage is always smaller (or equal) than the maximum voltage of the three phases.

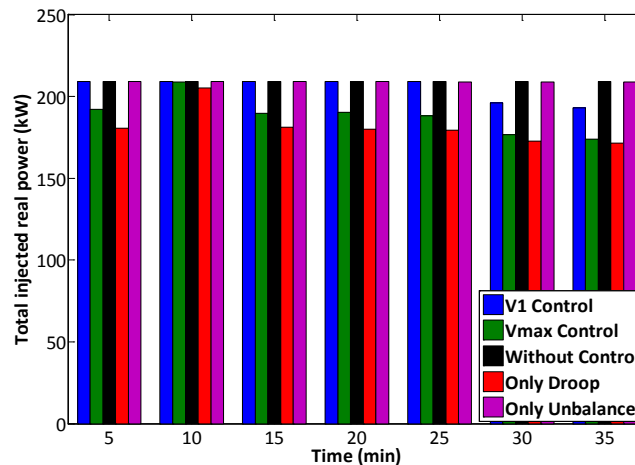


Fig. 5.32: Total inverter injected power for different control schemes vs time

The total power losses of the examined network are presented in Fig. 5.33 for the different control schemes. In this case there is no clear pattern which can adequately describe the network losses. This is due to the fact that the total load does not remain constant but changes every five minutes, following the given time series pattern. Thus, the total generated power as well as the total consumption varies among the different time instants. Generally, it can be concluded that both *V1 Control* and *Vmax Control* always manage to reduce total losses. On the other hand *Only Droop* and *Only Unbalance* control do not have a specific pattern and their performance depends highly on the specific network loading conditions.

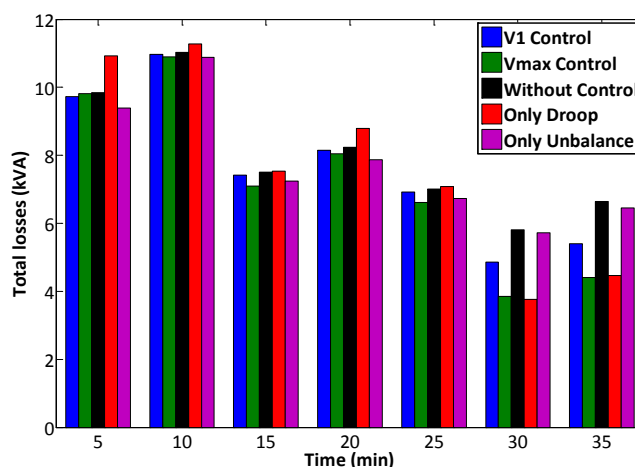


Fig. 5.33: Total apparent power losses for different control schemes vs time

INCREASE – *Increasing the penetration of renewable energy sources in the distribution grid by developing control strategies and using ancillary services*
 D3.1 - Dynamic equivalent models for the simulation of controlled DRES

5.4. Test case 4 – Energienetze Steiermark pilot installation

The configuration of the pilot installation of Energienetze Steiermark is considered next, as shown in Fig. 5.34. The LV network consists of two typical MV/LV distribution transformers with an aggregated load given in Table 5-9. The existing network configuration includes 15 single-phase conventional inverters distributed in the different phases of the installation. The specific installation has been selected because it provides flexibility on the reallocation of the existing inverters in different phases, to create asymmetries and also offers the opportunity to replace existing single phase with controlled 3phase inverters. In the examined configuration 9 single phase inverters are considered to be connected to phase A, whereas 2 3phase controllable inverters are installed in 7th and 10th floor cabinets. Their rated power is shown in Tables 5-10 and 5-11, respectively. Single phase inverters are operating at their rated values of Table 5-10, with leading power factors. One time instant is examined, although this can be extended in time since corresponding data are expected to be available by measurements.

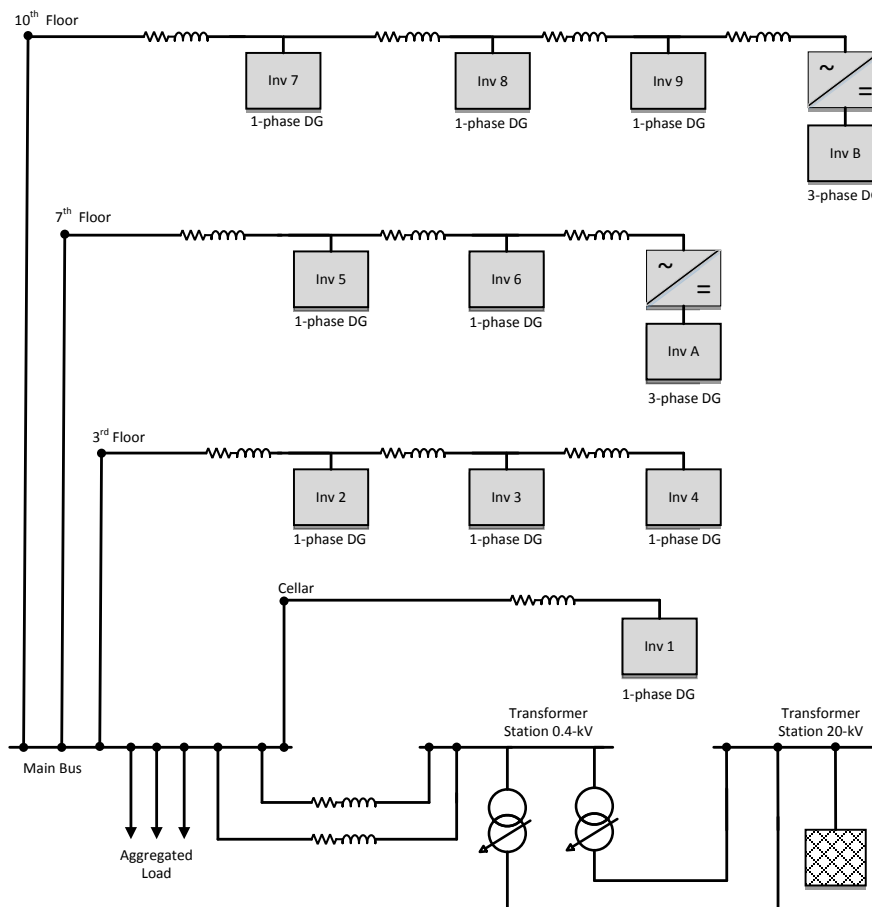


Fig. 5.34: Energienetze Steiermark network topology

INCREASE – Increasing the penetration of renewable energy sources in the distribution grid by developing control strategies and using ancillary services

D3.1 - Dynamic equivalent models for the simulation of controlled DRES

Table 5-9: Total aggregated load at Main Bus

	Real power (kW)	Reactive power (kVAr)
Phase A	44.676	13.59
Phase B	60.26	15.376
Phase C	57.96	13.723

Table 5-10: Rated powers of single-phase conventional inverters

	Real power (kW)	Reactive power (kVAr)
Inv 1	3.15	1.525
Inv 2	3.15	1.525
Inv 3	3.15	1.525
Inv 4	3.6	1.743
Inv 5	3.6	1.743
Inv 6	7.2	3.4868
Inv 7	7.2	3.4868
Inv 8	3.42	1.6563
Inv 9	3.42	1.525

Table 5-11: Rated powers of three-phase controllable inverters

	Rated Power (kVA)
Inv A	6.5
Inv B	24

5.4.1. Investigation of different control schemes

The two versions of Local Control are compared to the other traditional methods, as described previously. In Figs. 5.35 and 5.36 the total injected real power of the two 3phase controllable inverters and the total network power losses are presented, respectively. The *Without Control* and *Only Unbalance* methods inject the total rated power of the 2 three-phase inverters, since droop control mechanism is not invoked. The *V1 Control* also injects the same amount, since no real power curtailment is applied on the two controllable inverters. On the other hand, the *Vmax Control* and the *Only Droop* techniques curtail the total injected real power, resulting consequently to less power losses compared to the other methods.

INCREASE – Increasing the penetration of renewable energy sources in the distribution grid by developing control strategies and using ancillary services
D3.1 - Dynamic equivalent models for the simulation of controlled DRES

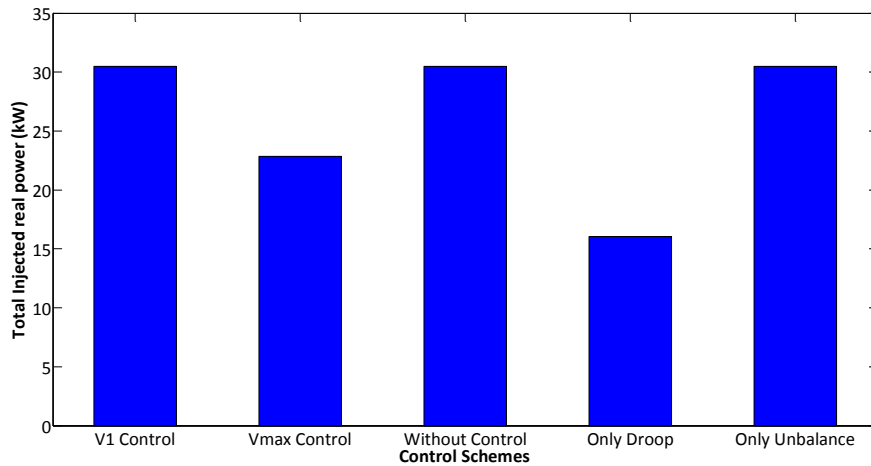


Fig. 5.35: Total inverter injected power for different control schemes

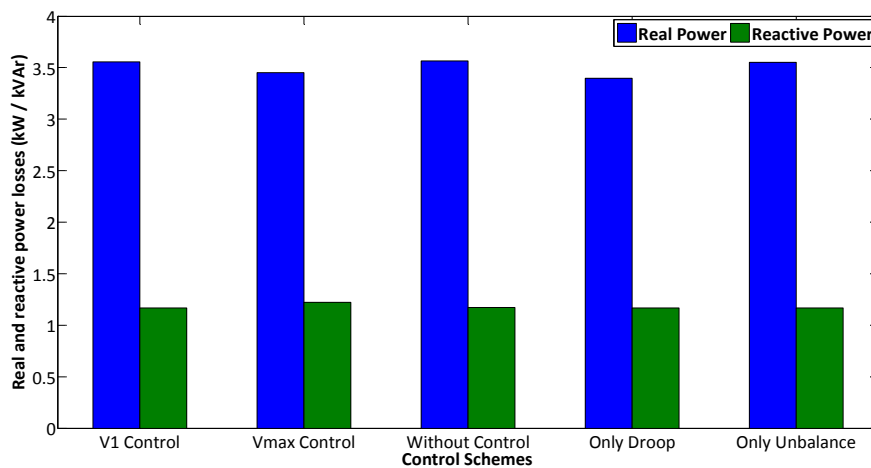


Fig. 5.36: Total power losses for different control schemes

The voltage profiles of the positive-sequence for the different control schemes is presented in Fig. 5.37. The voltages at buses “7th Floor” and “10th Floor” are mostly affected by the different control techniques, since the two 3phase controllable inverters are directly connected to these buses. Similar to the results of the previous test cases, the *Only Droop* control reduces the voltage levels of the positive-sequence, but also deteriorates both voltage unbalance factors in Fig. 5.38 and Fig. 5.39. On the other hand, the two versions of Local Control generally provide more acceptable results for both the positive-sequence voltage and the two voltage unbalance factors.

INCREASE – Increasing the penetration of renewable energy sources in the distribution grid by developing control strategies and using ancillary services
 D3.1 - Dynamic equivalent models for the simulation of controlled DRES

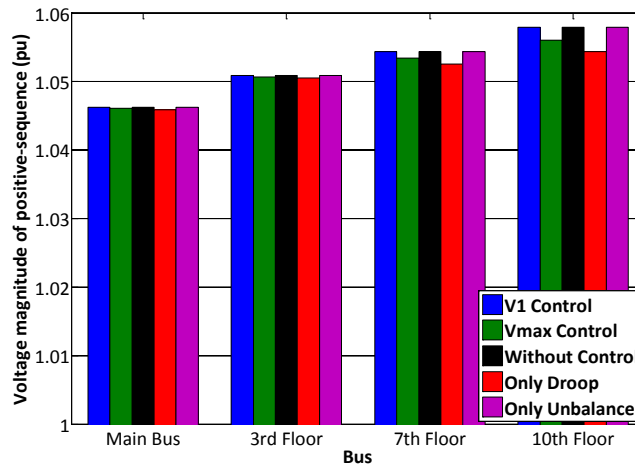


Fig. 5.37: Positive-sequence voltage levels for different control schemes

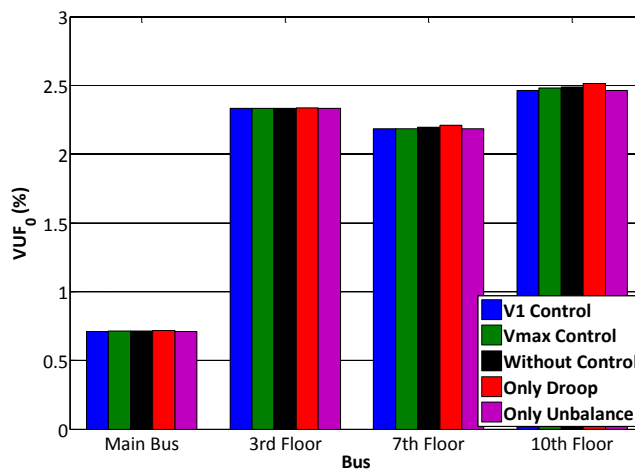


Fig. 5.38: Voltage unbalance factor of zero-sequence for different control schemes

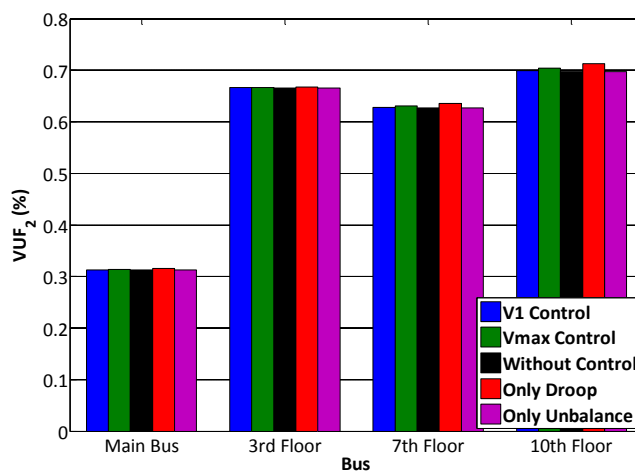


Fig. 5.39: Voltage unbalance factor of zero-sequence for different control schemes

INCREASE – *Increasing the penetration of renewable energy sources in the distribution grid by developing control strategies and using ancillary services*

D3.1 - Dynamic equivalent models for the simulation of controlled DRES

6. Conclusion

In this report, the grid simulation part including the controlled inverters of the INCREASE simulation platform is presented. The analysis starts with the description of the most common practice in the simulation of distribution networks and their classification into distinct categories, according to the adopted solution methods. The technical and numerical difficulties of each approach are analyzed, and the requirements for a new simulation platform are set, to provide multiple, combined simulation capabilities for extended distribution grids and smart grids, including controllable DRESs.

The properties of the INCREASE simulation platform are introduced, and the overall structure is thoroughly described. The report focuses on the features of GUI and on the software tools needed for the implementation of the core solution algorithm. The proposed scheme is demonstrated in various examples and is further compared with other conventional simulation software packages, revealing its superior performance in terms of accuracy, numerical stability and efficiency.

The Local Control of Deliverable D2.4 is successfully incorporated in the INCREASE simulation platform. The implemented control is slightly modified with the insertion of an integral term in the power output of the controlled inverters. This term enhances the numerical stability of the calculation procedure, without altering the performance of the system under study and the accuracy of the corresponding power flow results.

Two different implementations of the Local Control are considered and further demonstrated in various test cases including fictitious representative networks as well as two of the project pilot installations. Results are compared with the corresponding by conventional control methods, whereas a detailed investigation of the numerical performance is also performed. Both implementations of Local Control prove to be quite effective in both overvoltage and voltage unbalance mitigation, while also presenting smaller power curtailment of the injected power of the DG units, compared to the other conventional control schemes. Between the two implementations of the Local Control, using the maximum voltage for the droop control and for the calculation of the damping conductance leads to higher power curtailment, since it imposes more strict criteria than the case where the corresponding positive-sequence voltage is used.

The provided results show that the Local Control implementation in the INCREASE software platform can be applied to both LV and MV distribution grids, for variable time frames including variable load and generation data provided by the DSO. In all examined cases the INCREASE simulation platform performed with remarkably high speed and

INCREASE – *Increasing the penetration of renewable energy sources in the distribution grid by developing control strategies and using ancillary services*

D3.1 - Dynamic equivalent models for the simulation of controlled DRES

accuracy, while no numerical stability problems have been detected. Next versions of the platform will include additional control features, such as uniform power curtailment and the implementation of multi-agent systems.

INCREASE – *Increasing the penetration of renewable energy sources in the distribution grid by developing control strategies and using ancillary services*

D3.1 - Dynamic equivalent models for the simulation of controlled DRES

References

- [1] R. F. Arritt and R. C. Dugan, "Distribution system analysis and the future smart grid," *IEEE Trans. Ind. Appl.*, vol. 47, no. 6, pp. 2343-2350, 2011.
- [2] R. C. Dugan, R. F. Arritt, T. E. McDermott, S. M. Brahma, and K. Schneider, "Distribution system analysis to support the smart grid," in *Proc. IEEE Power Energy Soc. Gen. Meeting*, 2010.
- [3] T. L. Vandoorn, B. Meersman, J. D. M. De Kooning, and L. Vandeveldel, "Transition from islanded to grid-connected mode of microgrids with voltage-based droop control," *IEEE Trans. Power Syst.*, vol. 28, no. 3, pp. 2545-2553, 2013.
- [4] <http://www.mathworks.com/products/simpower/>
- [5] R. C. Dugan and T. E. McDermott, "An open source platform for collaborating on smart grid research," in *Proc. IEEE Power Energy Soc. Gen. Meeting*, 2011.
- [6] X.-P. Zhang, "Fast three phase load flow methods," *IEEE Trans. Power Syst.*, vol. 11, no. 3, pp. 1547-1553, 1996.
- [7] T. Demiray, G. Andersson, and L. Busarello, "Evaluation study for the simulation of power system transients using dynamic phasor models," in *Proc. IEEE/PES Transmission and Distribution Conf. Expo.*, 2008.
- [8] http://www.neplan.ch/html/e/e_home.htm
- [9] D. Bică, C. Moldovan, and M. Muji, "Power engineering education using NEPLAN software", in *Proc. 43rd Int. Univ. Power Eng. Conf.*, 2008.
- [10] <http://sourceforge.net/projects/electricdss/>
- [11] K. A. Birt, J. J. Graff, J. D. McDonald, and A. J. El-Abiad, "Three phase load flow program," *IEEE Trans. Power App. Syst*, vol. 95, no. 1, pp. 59-65, 1976.
- [12] R. M. Ciric, A. P. Feltrin, and L. F. Ochoa, "Power flow in four-wire distribution networks – General approach," *IEEE Trans. Power Syst.*, vol. 18, no. 4, pp. 1283-1290, 2003.
- [13] F. F. Wu and A. Monticelli, "Critical review of external network modelling for online security analysis", *Int. J. Elec. Power Energy Syst.*, vol. 5, no. 4, pp. 222-235, 1983.
- [14] K. Kato, "External network modelling – Recent practical experience," *IEEE Trans. Power Syst.*, vol. 9, no. 1, pp. 216-228, 1994.
- [15] J. V. Milanovic, K. Yamashita, S. M. Villanueva, S. Z. Djokic, and L. M. Korunovic, "International industry practice on power system load modeling," *IEEE Trans. Power Syst.*, vol. 28, no. 3, pp. 3038-3046, 2012.
- [16] IEEE Task Force on Load Representation for Dynamic Performance, "Standard load models for power flow and dynamic performance simulation," *IEEE Trans. Power Syst.*, vol. 10, no. 3, pp. 1302-1313, 1995.

INCREASE – *Increasing the penetration of renewable energy sources in the distribution grid by developing control strategies and using ancillary services*

D3.1 - Dynamic equivalent models for the simulation of controlled DRES

- [17] P. N. Papadopoulos, T. A. Papadopoulos, and G. K. Papagiannis, "Dynamic modelling of a microgrid using smart grid technologies," in *Proc. 47th Int. Univ. Power Eng. Conf.*, 2012.
- [18] P. N. Papadopoulos, T. A. Papadopoulos, G. K. Papagiannis, P. Crolla, A. J. Roscoe, and G. M. Burt, "Modeling of distributed energy resources using laboratory-experimental results," in *Proc. 48th Int. Univ. Power Eng. Conf.*, 2013.
- [19] P. N. Papadopoulos, T. A. Papadopoulos, P. Crolla, A. J. Roscoe, G. K. Papagiannis, and G. M. Burt, "Black-box dynamic equivalent model for microgrids using measurement data," *IET Gener., Trans. & Distrib.*, vol. 8, no. 5, pp. 851-861, 2014.
- [20] P. N. Papadopoulos, T. A. Papadopoulos, P. Crolla, A. J. Roscoe, G. K. Papagiannis, and G. M. Burt, "Measurement-based analysis of the dynamic performance of microgrids using system identification techniques," *IET Gener., Trans. & Distrib.*, early access.
- [21] J. F. Dopazo, M. H. Dwarakanath, J. J. Li, and A. M. Sasson, "An external system equivalent model using real-time measurements for system security evaluation," *IEEE Trans. Power App. Syst.*, vol. 96, no. 2, pp. 431-446, 1977.
- [22] B. Meersman, B. Renders, L. Degroote, T. Vandoorn, and L. Vandevelde, "Three-phase inverter-connected DG-units and voltage unbalance," *Elec. Power Syst. Res.*, vol. 81, pp. 899-906, 2011.
- [23] B. Renders, W. R. Ryckaert, K. De Gussemé, K. Stockman, and L. Vandevelde, "Improving the voltage dip immunity of converter-connected distributed generation units," *Renewable Energy*, vol. 33, pp. 1011-1018, 2008.
- [24] B. Renders, K. De Gussemé, W. R. Ryckaert, and L. Vandevelde, "Converter-connected distributed generation units with integrated harmonic voltage damping and harmonic current compensation function," *Elec. Power Syst. Res.*, vol. 79, pp. 65-70, 2009.
- [25] T. L. Vandoorn, B. Meersman, L. Degroote, B. Renders, and L. Vandevelde, "A control strategy for islanded microgrids with DC-link voltage control," *IEEE Trans. Power Del.*, vol. 26, no. 2, pp. 703-713, 2011.
- [26] V. M. A. M. Mansoor, P. H. Nguyen, and W. L. Kling, "An integrated control for overvoltage mitigation in the distribution network," in *IEEE PES Innov. Smart Grid Tech.*, 2014.
- [27] <http://jade.tilab.com/>
- [28] <http://inet.omnetpp.org/>
- [29] <http://www.mathworks.com/>
- [30] <http://smartgrid.epri.com/SimulationTool.aspx>
- [31] <http://faraday1.ucd.ie/psat.html>